Performance Evaluation of Massive MIMO-NOMA using Linear Receivers for 5G and Beyond

Derartu Merga Gobena

A Thesis Submitted to

The Department of Electronics and Communication Engineering

School of Electrical Engineering and Computing

Presented in Partial Fulfillment of the Requirement for the Degree of Master's in Electronics and Communication Engineering

Office of Post Graduate Studies

Adama Science and Technology University

Junly 2023

Adama Ethiopia

Performance Evaluation of Massive MIMO-NOMA using Linear Receivers for 5G and Beyond

Derartu Merga Gobena

Major Advisor:- Dr. Ram Sewak Singh (PhD)

Co-Advisor:- Mr. Tadesse Hailu

A Thesis Submitted to

The Department of Electronics and Communication Engineering

School of Electrical Engineering and Computing

Presented in Partial Fulfillment of the Requirement for the Degree of Master's in Electronics and Communication Engineering

Office of Post Graduate Studies

Adama Science and Technology University

Junly 2023

Adama, Ethiopia

APPROVAL PAGE of M.SC. THESIS

We, the advisors of the thesis entitled **"Performance Evaluation of Massive MIMO-NOMA using Linear Receivers for 5G and Beyond"** and developed by Derartu Merga Gobena, hereby certify that the recommendation and suggestions made by the board of examiners are appropriately incorporated into the final version of the thesis.

Dr. Ram Sewak Singh	____________________	______________
Major Advisor	Signature	Date
Mr. Tadesse Hailu	____________________	______________
Co-Advisor	Signature	Date

We, the undersigned members of the board of Examiners of the thesis by Derartu Merga Gobena have read and evaluated the thesis entitled **"Performance Evaluation of Massive MIMO-NOMA using Linear Receivers for 5G and Beyond"** and examined the candidate during open defense. This is, therefore, to certify that the thesis is accepted for full fulfillment of the requirement of the degree of Master of Science in Electronics and Communication engineering.

____________________	____________________	______________
Chairperson	Signature	Date
____________________	____________________	______________
Internal Examiner	Signature	Date
____________________	____________________	______________
External Examiner	Signature	Date

Finally, approval and acceptance of the thesis is contingent upon submission of its final copy to the Office of Postgraduate Studies (OPGS) through the Department Graduate Council (DGC) and School Graduate Committee (SGC).

____________________	____________________	______________
Department Head	Signature	Date
____________________	____________________	______________
School Dean	Signature	Date
____________________	____________________	______________
Office of Postgraduate Studies, Dean	Signature	Date

DECLARATION

I hereby declare that this Master's Thesis entitled "**Performance Evaluation of Massive MIMO-NOMA using Linear Receivers for 5G and Beyond"** is my work and has not been submitted to any university for the award of any academic degree, diploma or certificate. The references used in this thesis are duly recognized by proper citations.

Derartu Merga Gobena	________________	______________
Name of Student	Signature	Date

RECOMMENDATION

We, the advisors of this thesis, hereby certify that we have read the revised version of the thesis entitled **"Performance Evaluation of Massive MIMO-NOMA using Linear Receivers for 5G and Beyond''** prepared under our guidance by Derartu Merga Gobena submitted in full fulfillment of the requirements for the degree of Masters of Science in Electronics and Communication Engineering. Therefore, we recommend the submission of revised version of the thesis to the department following the applicable procedures.

______________________	______________	______________
Major Advisor	Signature	Date
______________________	______________	______________
Co-advisor	Signature	Date

ACKNOWLEDGEMENT

Firstly, I would like to express my gratitude to God for his mercies and blessings that allowed me to successfully complete this thesis. I want to thank my advisor, Dr. Ram Sewak Singh (Ph.D.), for his encouragement, support, and willingness to sacrifice his valuable time to guide me in the right direction. Without his assistance, it would have been impossible for me to achieve the ultimate goal of this thesis. He was always available to help me whenever I encountered obstacles in my research work.

I also want to extend my sincere appreciation to my co-advisor, Mr. Tadesse Hailu (M.Sc.), for his continuous support, patience, motivation, and enthusiasm throughout my M.Sc. research. His guidance was instrumental in helping me conduct my research and write this thesis.

Furthermore, I would like to thank Adama Science and Technology University (ASTU) and all members of the School of Electrical Engineering and Computing (SoEEC), particularly the Electronics and Communication Engineering department, for providing an excellent educational and research environment. I am grateful to all the students in the Communication Engineering division who shared their knowledge with me.

Finally, I am grateful to my family for always supporting me and giving me the freedom to pursue my goals without feeling pressured.

Table of Contents

LIST OF TABLES

LIST OF FIGURES

ACRONYM

3GPP	3rd Generation Partnership Project
4G	Fourth Generation
AF	Amplified-and-Forward
AMPS	Advance Mobile Phone Service AMPS
AWGN	Additive White Gaussian Noise
BDMA	Beam Division Multiple Access
BS	Base Station
CDMA	Code Division Multiple Access
CDMA	Code Division Multiple Access
CSI	Channel State Information
DF	Decoded-and-Forward
EE	Energy Efficiency
FBMC	Filter Bank Multi Carrier
FDMA	Frequency Division Multiple Access
HetNets	Heterogeneous Networks
HTC	Human-Type Communication
IEEE	Institute of Electrical and Electronics Engineers
IP	Internet Protocol
LMMSE	Linear Minimum Mean-Square Error
LTE	Long-Term Evolution
MF	Matched-Filter
MIMO	Multiple-Input Multiple-Output
mMIMO	Massive Multiple-Input Multiple-Output

MMSE	Minimum Mean Square Error
MMSE	Minimum Mean-Square Error
mMTC	Massive Machine Type Communication
mm-Wave	Millimeter Wave
MRC	Maximum Ratio Combining
MRC	Maximum Ratio Combining
MTC	Machine-Type Communication
MU-MIMO	Multi-User MIMO
NOMA	Non-Orthogonal Multiple Access
OFDMA	Orthogonal Frequency Division Multiple Access
OMA	Orthogonal Multiple Access
PIC	Parallel Interference Cancellation
PPP	Poisson Point Process
PSK	Phase Shift Keying
QAM	Quadrature Amplitude Modulation
QoS	Quality of Service
RS	Relay Station
SC	Superposition Coding
SE	Spectral Efficiency
SIC	Successive Interference Cancellation
SMS	Short Message Service
SNR	Signal-to-Noise Ratio
SQP	Sequential Quadratic Programming
TDMA	Time Division Multiple Access

TDMA	Time Division Multiple Access
UP	User Pairing
ZF	Zero Forcing

ABSTRACT

The ever-increasing demand for higher data rates and reliable wireless communication has led to the exploration of new technologies and techniques to improve spectral efficiency. Traditional wireless communication systems, such as orthogonal frequency-division multiplexing (OFDM) and time-division multiplexing (TDM), have limitations in terms of spectral efficiency, particularly in scenarios where the number of users is high. To overcome this limitation, new techniques such as non-orthogonal multiple access (NOMA) have been proposed. To further improve the spectral efficiency of wireless communication systems, massive MIMO and NOMA can be combined to create massive MIMO NOMA systems. In such systems, multiple antennas are used to serve multiple users using NOMA techniques. This paper presents a performance analysis of massive MIMO NOMA systems with different linear receivers. The channel model used is a Rayleigh fading channel, and the performance is evaluated for K=N and K>N scenarios. The complexity of the receivers is measured in terms of the average number of matrix inversions and the average number of successive interference cancellation (SIC) operations. The linear receivers considered are MRC, MRC with SIC (MRC-SIC), ZF, MMSE, ZF ZF-PIC, and MMSE with PIC/SIC and others. From the analysis in the case of K=N, which refers to the scenario where the number of users is equal to the number of antennas, the best performing linear receiver is MMSE-PIC. However, in the scenario where K>N, the best performing linear receiver is MRC-SIC. To improve the outage probability of the well performing receiver (MMSE_PIC), MMSE_PIC_QR which uses QR decomposition principle on MMSE detector matrix is also proposed.

Keywords: Massive MIMO, NOMA, ZF, MRC, MMSE, SIC, PIC

CHAPTER ONE

1. INTRODUCTION

1.1 Background of the Study

Initially, mobile communication technology was limited to basic voice communication capabilities. With the advent of the 2G, both voice and data services were made available. However, the third generation proved to be a breakthrough, providing subscribers with a variety of data services that involve the transmission and processing of digital information, including but not limited to accessing the internet via mobile devices, conducting virtual meetings through video conferencing, and using various multimedia applications. This development resulted in a significant expansion of the telecommunications industry. To meet the growing demand, the industry shifted to the fourth generation, commonly known as 4G, which added even additional, enhanced functionalities added to the current voice and 3G services. 4G offers users ultra-broadband mobile internet access, with much faster data transfer speeds. The standard emphasizes improved lossless reception, seamless mobile internet with IP interoperability, and faster information exchange(Agrawal et al., 2015).

The forthcoming 5G system must outperform earlier generations in terms of speed and capacity while also accommodating brand-new usage scenarios with a wide range of needs, such as various machine-type communication methods. In order to achieve this, the METIS project has developed a 5G system model that consists of three generic 5G services: ultra-high-speed mobile broadband, huge machine-type communication, and MTC with ultra-high reliability. These services are supported by four key enablers: a lean system control plane, a dynamic radio access network, localized contents , and traffic flows, and a spectrum toolbox (Tullberg et al., 2016), describe these important system-level 5G features, which are enabled by the concept and are essential in meeting the wide-ranging requirements of the 5G system.

The transition from 1G to 4G communication technologies involved the use of various core channel accessing technologies, such as frequency division multiple access (FDMA), time division multiple access (TDMA), code division multiple access (CDMA), and orthogonal frequency division multiple access (OFDMA). These accessing modes played a crucial role in the evolution of the technologies(Iswarya & Jayashree, 2021). To decrease the chance of fading and to reduce interference, Multiple-Input Multiple-Output (MIMO) technology is integrated with Non-Orthogonal Multiple Access (NOMA) in a system called MIMO-NOMA. This combination enables the use of multiple antennas in transmission, improving the overall performance of the system and canceling out the effects of interfering signals.

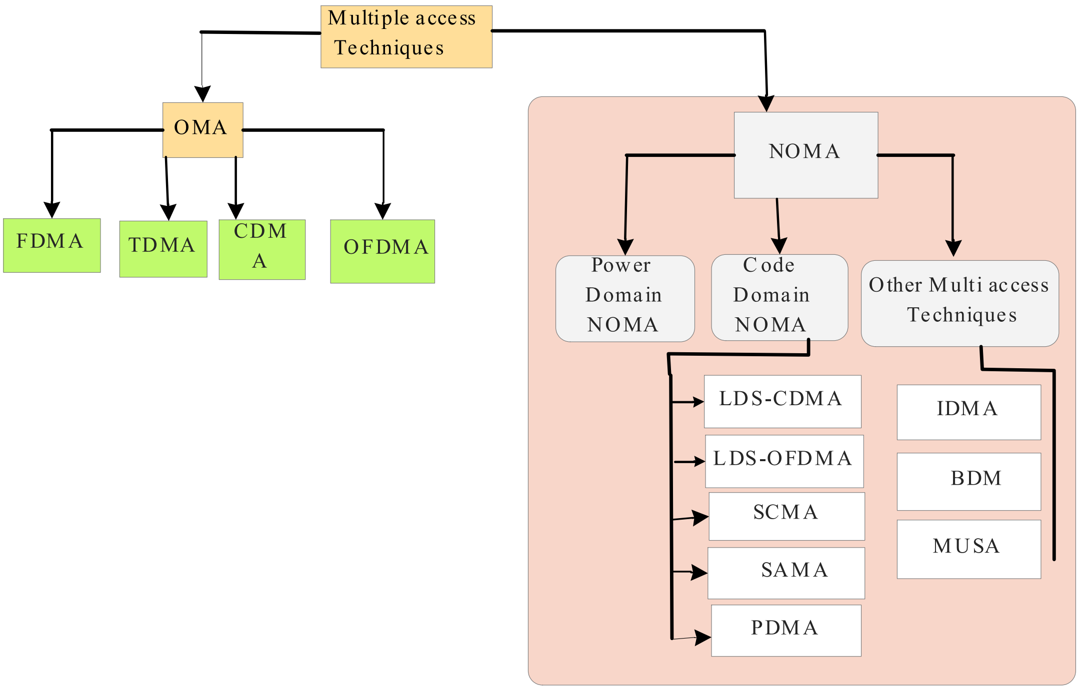

Figure 1.1: Classification of Multiple Access Techniques (Iswarya & Jayashree, 2021)

The next ten years are expected to see a 1000-fold growth in mobile data traffic, which the fifth generation (5G) cellular technology is designed to handle. The need to significantly increase spectral efficiency in comparison to current networks is a crucial challenge for 5G networks. Non-orthogonal multiple access (NOMA), one of the major methods to raise the per-cell spectral efficiency, has drawn a lot of interest from academics. Massive MIMO, which makes use of base stations (BSs) with numerous antennas, is another important technology. The initial 5G standard release has now been completed and includes a number of capabilities, such as massive MIMO and NOMA. From the First Generation (1G) through the Fourth Generation (4G) Long-Term Evolution (LTE), traditional wireless communications systems were primarily created and optimised to serve Human-Type Communication (HTC), such as voice calls, text messages, and mobile internet. Machine-Type Communications (MTC), a crucial enabler for the Internet of Things revolution, has also been supported in the most recent iterations of 4G LTE and Fifth Generation (5G) New Radio (NR) (Dawy et al., 2017).

Improving spectral efficiency within specified energy constraints is a crucial consideration for future wireless communications to meet the growing transmission needs of wireless devices. (H. Wang et al., 2021), propose a wireless-powered relay station (RS) in a non-orthogonal multiple access (NOMA)-based cognitive radio network and analyze the system outage performance under amplified-and-forward (AF) and decoded-and-forward (DF) cooperative transmission modes. The aim is to enhance the spectral efficiency of communication systems without increasing energy consumption. In massive multiple-input multiple-output (MIMO) systems, linear detectors such as maximum ratio combining (MRC), zero forcing (ZF), or minimum mean square error (MMSE) can achieve optimal results. MRC receivers maximize the received signal power while ignoring interference from other users, making them more suitable for lower transmission powers(Beiranvand & Meghdadi, 2018).

Compared to other linear detectors such as zero forcing (ZF) and maximum ratio combining (MRC), the minimum mean square error (MMSE) detector plays the most significant role in improving the performance of Nakagami-m fading channels. While MRC has the advantage of enabling a distributed per-antenna implementation of the detector, ZF outperforms MRC due to its ability to cancel out interference created between the antennas of the transmitter and receiver(Uddin et al., 2014).

1.1.1 Motivation

With the increasing demand for high data rates and low latency in wireless communication systems, researchers and engineers are exploring new technologies and techniques to improve the efficiency and performance of communication systems. Massive MIMO and NOMA are two emerging technologies that have shown promise in addressing these demands. Beyond 5G technologies are the next generation of wireless communication systems that are expected to provide even higher data rates and lower latency than current 5G systems. The performance evaluation of massive MIMO NOMA with linear receivers beyond 5G can shed light on the potential of these technologies and their suitability for future wireless communication systems. Linear receivers are a simple and computationally efficient solution for massive MIMO and NOMA systems, making them attractive for practical implementations. Evaluating the performance of linear receivers in massive MIMO NOMA can provide insights into practical solutions that can balance performance and complexity.

1.2 Statement of the problem

Beyond 5G networks are being developed to provide a wide range of extremely demanding services and applications. This is done by pushing network capabilities to deliver extreme performance, including the support of massively linked devices in the context of machine type communication (MTC). In the upcoming years, it is anticipated that MTC network requirements will increase in rigor. In some cases of mMTC (massive Machine Type Communication), it may not be feasible to equip receivers with a significant number of antennas due to factors such as cost, size, or power constraints. As a result, the number of active devices in a given time slot could exceed the number of available antennas. Even if devices transmitting in higher frequency bands can be served by utilizing a Massive MIMO network, using massive MIMO will be very costly. So, beyond the 5G network using massive MIMO with a manageable number of antennas by combining it with the NOMA technique will be a solution. The integration of massive Multiple-Input Multiple-Output (mMIMO) techniques with NOMA employing either Successive Interference Cancellation (SIC) or Parallel Interference Cancellation (PIC) decoding can result in the highest performing receivers that offer optimal spectral efficiency in the decoding of multiple overlapping signals using SIC/PIC.

1.3 Objective of the Study

1.3.1 General objectives

The main objective of this thesis is to Evaluate the Performance of Massive MIMO-NOMA with Linear Receivers for 5G and Beyond.

1.3.2 Specific objective

The specific objectives of this research are: -

- To Compute the Outage probability based on the average number of correctly decoded device.
- To evaluate the spectral efficiency of different linear receivers with respect to signal to noise ratio.
- To analyze Comparison between the receivers that utilize SIC and PIC decoding schemes.
- To improve the performance of MMSE_PIC receivers with QR decomposition.

- To evaluate the computational complexity of different linear receiver like MRC, ZF and MMSE, MRC-SIC.

1.4 Significance of the Study

The advancement of cellular technology beyond fifth generation (5G) aims to accommodate the anticipated surge in mobile data traffic and the need for massive connectivity over the next decade. A crucial challenge for these future cellular networks is to substantially enhance the spectral efficiency compared to current networks. One of the primary technologies that can help attain this goal is the combination of non-orthogonal multiple access (NOMA) techniques that utilize either Successive Interference Cancellation (SIC) or Parallel Interference Cancellation (PIC) decoding with massive Multiple-Input Multiple-Output (MIMO) technology. Massive MIMO involves the use of base stations equipped with a large number of antennas, which allows for increased capacity and better reception quality. By combining these technologies, it is possible to achieve a higher level of spectral efficiency per cell, which is crucial for meeting the demands of future mobile communications.

1.5 Scope of the Study

The objective of this paper is to enhance the limited spatial multiplexing capabilities of multi-antenna techniques, which are inadequate for providing connectivity to a vast number of devices. The paper evaluates the performance of linear receivers that can deal with this situation by combining massive MIMO techniques with NOMA that utilizes either Successive Interference Cancellation (SIC) or Parallel Interference Cancellation (PIC) decoding. These linear receivers can perform dynamic ordering SIC/PIC decoding of multiple overlapping signals, even when the number of active devices exceeds that of receive antennas. Overall, this paper presents a promising analysis approach to improve the spatial multiplexing capabilities of wireless communication systems by utilizing advanced techniques while maintaining high spectral efficiency. Finally, the performance between different linear receivers will be evaluated. All evaluation will be done using MATLAB software communication tools.

CHAPTER TWO

2. LITERATURE REVIEW

2.1 Evolution of Wireless Technologies

During the early 1980s, the initial generation of mobile phone technology was created with a primary focus on voice services. Most of these systems were analog and relied on frequency modulation techniques for radio transmissions. These systems utilized frequency division multiple access (FDMA) and had a channel capacity of 30 KHz. The frequency band used for this technology was within the range of 824-894 MHz and was based on Advance Mobile Phone Service (AMPS)(Yiping & Yuhang, 2007).

The advent of the second generation of mobile communication systems represented a significant shift towards digital technology. This transition allowed for more efficient utilization of the available bandwidth, leading to improved call quality and enhanced capacity for data transmission. Although 2G systems were still primarily employed for voice communication, they also introduced some supplementary services such as SMS (Short Message Service) and email. There were two digital modulation schemes utilized in 2G systems: Time Division Multiple Access (TDMA) and Code Division Multiple Access (CDMA). TDMA splits each frequency channel into multiple time slots, enabling multiple users to share the same frequency band. On the other hand, CDMA employs a unique code to differentiate between different users, allowing multiple users to transmit and receive data simultaneously over the same frequency band. The typical frequency band used for 2G systems ranged from 850-1900 MHz. This range provided better coverage both indoors and outdoors, but it also required more cell towers to be installed in order to provide sufficient coverage (Li et al., 2009). In 2G systems, the GSM technology employed eight channels per carrier, with a gross data rate of 22.8 kbps (equivalent to a net rate of 13 kbps) in the full rate channel, and a frame duration of 4.6 milliseconds (ms). The second generation of mobile communication systems includes 2G, 2.5G, and 2.75G.

The introduction of the third generation (3G) of mobile communication services brought together high-speed mobile access and Internet Protocol (IP)-based services. 3G technology offered a range of key features such as wireless web access, multimedia services, email, and video conferencing.

The W-CDMA air interface standard for 3G was specifically designed for "always-on" packet-based wireless services, enabling computers, entertainment devices, and telephones to share the same wireless network and stay connected to the internet anytime and anywhere. 3G systems offered high data rates of up to 2 Mbps over a 5 MHz channel carrier width, depending on mobility and velocity, as well as high spectrum efficiency. The data rate supported by 3G networks varied based on the call environment, ranging from 144 kbps in satellite and rural outdoor settings to 384 kbps in urban outdoor settings, and up to 2 Mbps in indoor and low-range outdoor settings. The frequency band used for 3G technology was within the range of 1.8-2.5 GHz(Gupta & Jha, 2015).

4G technology is widely regarded as the successor to 2G and 3G standards, with Long-Term Evolution (LTE) Advanced proposed as the future 4G standard by the 3rd Generation Partnership Project (3GPP). 4G deployment is expected to offer users a secure IP-based solution for voice, multimedia, and data services with significantly higher data rates than previous generations, but with demanding Quality of Service (QoS) requirements. 4G networks are being developed to support applications such as wireless broadband access, MMS, video chat, mobile TV, HDTV content, and DVB (Glisic & Makela, 2006).

The deployment of the 5G wireless communication system is yet to take place. However, its design and deployment aim to increase system capacity and quality within the available frequency spectrum. The proposed 5G system features and architecture aim to achieve a frequency band of 3-300GHz and a data bandwidth of at least 1Gbps, with no limitations on user demands for the next 200 years. The 5G system will interconnect the entire wireless world through the Wireless Innovative System for Dynamic Operating Mega communications concept (WISDOM). It is expected to provide high data rates for Quality of Service (QoS) applications(Ghosh et al., 2019).

2.2 Introduction to 5G and beyond 5G

Due to the increasing user demand, 5G technology, which utilizes advanced access technologies such as Beam Division Multiple Access (BDMA) and Non-/Quasi-Orthogonal or Filter Bank Multi Carrier (FBMC) Multiple Access, is expected to replace 4G rapidly. The concept underlying BDMA technology becomes clearer when examining the interaction between the base station and mobile stations(Gupta & Jha, 2015).

5G networks are expected to offer faster speeds, lower latency, and increased capacity than previous generations of wireless networks. However, these new capabilities also introduce new security challenges. One of the main challenges is ensuring the confidentiality, integrity, and availability of user data by implementing strong encryption, authentication, and access control mechanisms. Another challenge is securing the increased complexity of 5G networks, such as the use of network slicing, edge computing, and a higher number of devices and endpoints that create potential attack surfaces. (Fang et al., 2018).

The faster data rates enabled by Beyond-5G wireless technologies pose an increased risk of data breaches and cyber-attacks, while their complexity makes them difficult to secure. As these technologies expand, they may introduce new potential attack surfaces that malicious actors could exploit. With the growth of the Internet of Things (IoT), securing the increasing number of devices and endpoints could create new challenges(Ruzomberka et al., 2023).

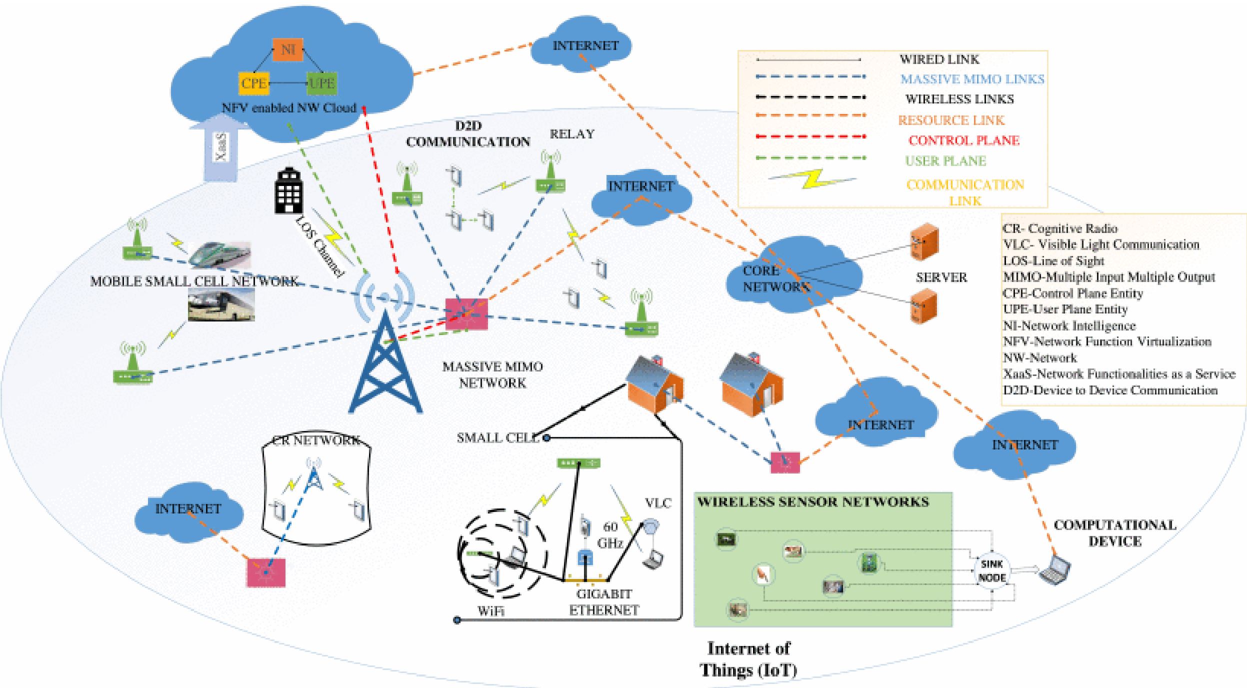

Figure 2.1: A general 5G cellular network architecture (Gupta & Jha, 2015)

2.3 Introduction to Massive MIMO

MIMO systems have become essential for current wireless systems, providing significant spectrum and energy efficiency. Before MIMO, single-input, single-output systems had poor throughput and could not support many users with high dependability. To meet market demand, novel MIMO technologies like single-user MIMO (SU-MIMO), multi-user MIMO (MU-MIMO), and network MIMO were developed. However, due to the significant increase in wireless users in recent years, these technologies are no longer sufficient to handle the trillions of bits of data that require efficient and reliable handling.

For future wireless access, Massive MIMO is currently the most promising sub-6 GHz physical-layer technology. The main idea behind this technology is to use large antenna arrays at base stations to serve many independent terminals simultaneously(Larsson & Van der Perre, 2017). Massive MIMO provides several benefits, including better support for multi-user MIMO (MU-MIMO), where a base station equipped with multiple antennas serves a group of single-antenna users who share the multiplexing gain. Additionally, MIMO technology is particularly useful in higher frequency bands, such as the millimeter wave (mm-Wave) band, where a single antenna has poor directivity and a wide radiation pattern. In 5G networks, high directivity is necessary, which can be achieved through antenna arrays without reducing the size of individual antenna elements. This is why massive MIMO technology has been developed (Shaikh & Kaur, 2019).

In the future, wireless base stations and access points will employ a large number of antennas for transmitting and receiving signals. To achieve such massive arrays in a flexible and scalable way, while minimizing power consumption and cost, a promising technology is the use of radiating metamaterial elements called metasurfaces. Metasurfaces are currently utilized as passive reflecting devices to assist conventional transceivers in controlling the propagation environment in wireless communication contexts.(Shlezinger et al., 2021). The suggested antenna is composed of a metasurface that features an array of resonant elements with subwavelength size. The resonant elements can be dynamically controlled to steer and shape the electromagnetic waves that the antenna transmits and receives.

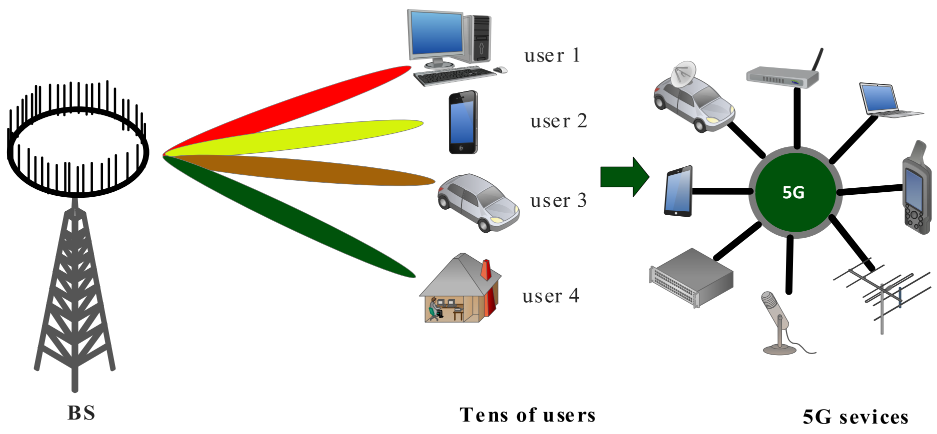

Figure 2.2: Massive MIMO system beamforming and its services (Albreem et al., 2021)

To improve beamforming efficiency and reduce interference, it may be necessary to divide the transmitter into sectors. When it comes to beamforming or large antenna arrays, the first thing that comes to mind is the impressive flexibility of directing a beam in a multi-user environment. However, a fully digital MIMO beamforming method may be costly despite offering the most beam steering flexibility. A better outcome can be achieved by combining beamforming approaches from the analog, digital, and RF domains, which provides less flexibility than a fully digital MIMO system but is more cost-effective(Jumaah & Qasim, 2022).

2.3.1 Advantage of Massive MIMO in 5G

The main advantages of massive MIMO technology are as follows(Wu, 2018):

(1) Massive MIMO systems exhibit remarkably low power consumption in their antennas. Therefore, the total transmitted power needed by each antenna has an inverse relationship with the number of antennas at a fixed total transmitting power. Similarly, as the number of antennas increases, the total transmitting power decreases at a certain signal-to-noise ratio. Consequently, the power requirement of each antenna decreases in direct proportion to the square of the number of antennas. This leads to a significant reduction in power consumption in massive MIMO systems.

(2) Massive MIMO systems exhibit the "channel hardening" phenomenon, where the channel matrix can be analyzed using the theory of random matrices as the number of antennas approaches infinity. In this scenario, the channel vectors tend to become orthogonal, and the singular values of the channel matrix follow a well-known asymptotic

distribution. Consequently, the most fundamental signal processing method can attain asymptotic perfection.

(3) Small-scale fading and thermal noise are mitigated in massive MIMO systems. Linear signal processing techniques can reduce the impact of these factors on system performance as the number of antennas increases. However, inter-cell interference is more significant than the effects of thermal noise and small-scale fading.

(4) Massive MIMO systems improve spatial resolution by increasing the number of base station antennas. This allows beamforming techniques to focus transmitted signals on a specific location in space, enabling the base station to distinguish between each user accurately. As a result, the spatial resolution is enhanced.

2.3.2 Challenges in massive MIMO

Apart from the challenges posed by MIMO technology, there are several other issues that must be addressed to implement massive MIMO technology. Although massive MIMO builds on the concepts of MIMO, it also presents unique problems and obstacles that must be overcome for it to be feasible. The figure 2.3 highlights some of the key challenges faced by massive MIMO systems.

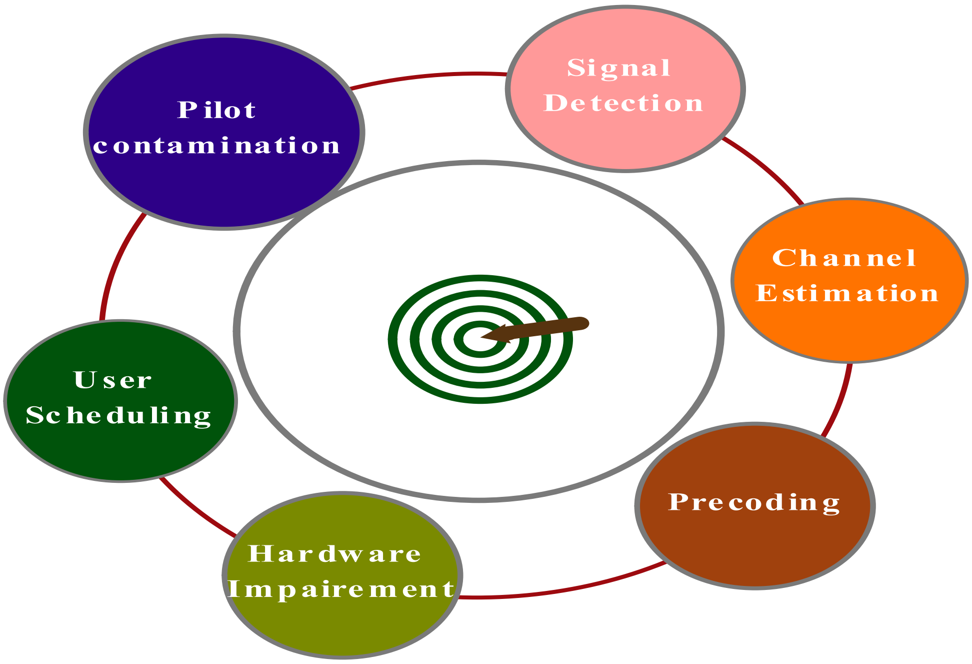

Figure 2.3: Challenges in massive MIMO deployment(Chataut & Akl, 2020)

Pilot contamination: Pilot contamination refers to the interference that arises during channel estimation when two or more users in the network are assigned the same pilot sequence.

Signal detection: Massive MIMO signal detection is necessary for estimating the transmitted signals from the signals received at the base station.

Channel estimation: The large number of antennas in massive MIMO systems can result in strong coupling between channels. This strong coupling, along with interference and noise caused by channel correlation, can make accurate channel estimation challenging.

Precoding: User interference poses a significant challenge for the precoding methods used in massive MIMO systems.

Hardware impairment: The probability of hardware imperfections or failures rises with more antennas, which might result in performance loss and decreased system throughput.

User scheduling: With a large number of users and antennas, the possible scheduling configurations that can be used may be extensive. This can complicate computations and make it difficult to identify the optimal scheduling arrangement.

2.4 NOMA concept and its role in 5G

Non-orthogonal multiple access (NOMA) is a unique approach to multiple-user access that differs from traditional schemes such as orthogonal multiple access. NOMA intentionally introduces intercell and/or intracell interference at the transmitter to enable non-orthogonal transmission. The receiver uses successive interference cancellation (SIC) techniques to decode the intended signal. Although the receiver's complexity is higher than that of orthogonal multiple access, NOMA can achieve higher spectral efficiency. The fundamental idea behind non-orthogonal access is to use a receiver with a more intricate design in exchange for increased spectral efficiency. Thanks to advances in chip processing technology, implementing the non-orthogonal access scheme has become possible(Hussain & Rasheed, 2020).

The exponential increase in the number of users has led to a rise in demand for higher data rates and connectivity. To fulfill these demands, new technological trends such as NOMA-assisted base stations (BS) can be adopted. However, the efficient utilization of resources in NOMA presents several challenges. Among these, the most significant challenge is resource management in NOMA-assisted fifth-generation (5G) and beyond-5G (B5G) networks (Ghafoor et al., 2022).

The ongoing progress in non-orthogonal multiple access (NOMA) is anticipated to bring significant enhancements to heterogeneous networks (HetNets) and enable wireless networks beyond the fifth-generation (5G). This study proposes an effective framework for optimizing user association and power control in NOMA-enabled HetNets. The issue of cellular device association and power control is specifically formulated as a non-convex optimization problem. The original problem is then broken down into two subproblems, each with successive interference cancellation (SIC) and various quality-of-service constraints. To efficiently solve the user association and power control subproblems, the dual theory and sequential quadratic programming (SQP) approaches are employed(Khan et al., 2021).

2.4.1 Uplink NOMA

In an uplink scenario, the equipment of each user (UE) transmits signals towards the base station (BS). The successive interference cancellation (SIC) technique is then employed at the BS to separate the signals of UEs with their respective power allocation coefficients.

In an uplink NOMA system, sharing spatial resources can enhance the system's overall capacity, but it can also lead to interference between users. To alleviate the performance degradation caused by this interference, two strategies can be employed: a set selection algorithm to decrease interference and an optimal power control scheme to maximize the sum capacity. These strategies aim to strike a balance between maximizing the system's capacity and minimizing interference between users(Kim et al., 2015).

2.4.2 Downlink NOMA

In the downlink situation, the base station (BS) applies the superposition coding (SC) technique to multiplex signals with varying power allocation coefficients. At the receiver end, the successive interference cancellation (SIC) technique is utilized to segregate interfering signals. The power allocation coefficients are allocated based on the channel conditions of users, with high power assigned to poor channel condition users and low power assigned to better channel condition users(Budhiraja et al., 2021).

Downlink Non-Orthogonal Multiple Access (NOMA) utilizes superposition coding at the base station and employs successive interference cancellation decoding at the user end. To ensure fair treatment of users, NOMA allocates more power to those with weaker channel conditions. However, applying NOMA to all users jointly can be challenging due to additional system overhead for channel feedback coordination and error propagation. Thus, the concept of user pairing (UP) has emerged, where users are grouped into multiple clusters, and NOMA is utilized within each cluster. In MIMO-NOMA systems, user pairing significantly impacts the sum rate gain. When employing zero-forcing precoding in a two-user cluster, the weaker user's channel conditions do not affect the stronger user's rate. Therefore, the stronger user should be chosen first to form a cluster, and the weaker user selected to optimize performance by minimizing intra- and inter-cluster interference. To reduce interference, it is beneficial to group users with distinct channel gains but highly correlated channels. Large-gain differences ensure effective NOMA, while high correlation eliminates inter-cluster interference. Careful selection of users for clusters can enhance overall MIMO-NOMA system performance and increase sum rate gains(Islam et al., 2018).

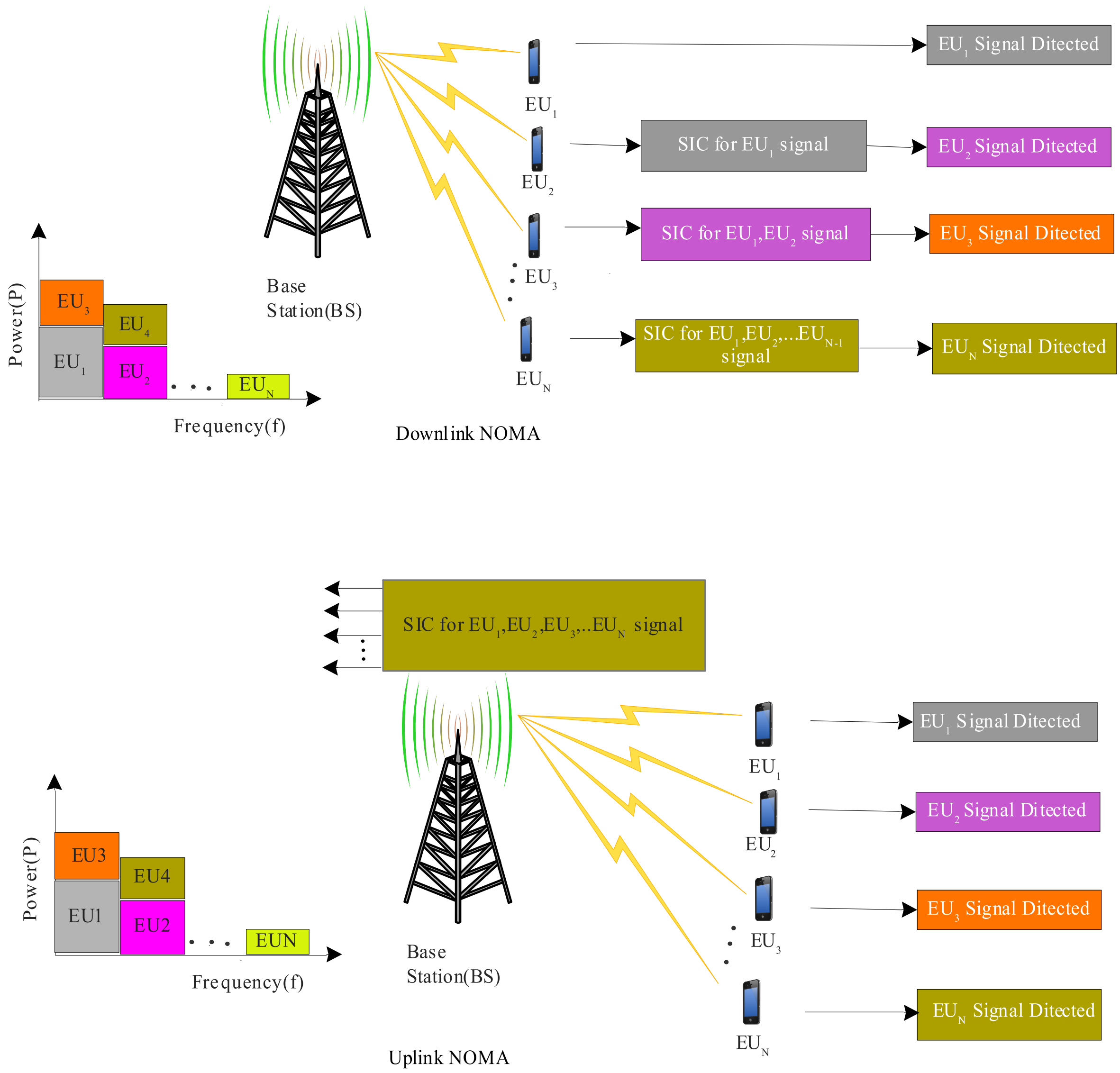

Figure 2.4: Downlink and uplink NOMA (Budhiraja et al., 2021)

2.4.3 Key Distinctions Between Uplink and Downlink NOMA

The most significant differences between uplink and downlink Non-Orthogonal Multiple Access (NOMA) are as follows(Tabassum et al., 2017):

1) Implementation Complexity: To enable downlink NOMA, it is crucial to employ advanced multi-user detection and interference cancellation techniques at every user's receiver. However, this can be challenging due to the limited processing capabilities of these receivers. In comparison, implementing these techniques on a centralized entity, such as the Base Station (BS), is more practical for the uplink.
2) Intra-cell/Intra-cluster Interference: In the downlink, intracell interference affects a user's own channel, creating strong interference for users with strong downlink

channels. This is due to the strong interfering channel and relatively high transmit powers assigned to weak channel users. In contrast, users with weak downlink channels experience low interference due to their weak channel and the low transmit powers assigned to strong channel users. Therefore, users with strong downlink channels are more susceptible to intracell interference, which is resolved by using successive interference cancellation (SIC) at the users' end. In the uplink, the base station (BS) receives transmissions from all users simultaneously, and intra-cell interference depends on other users' channel characteristics within the cluster. Weak channel users are more susceptible to strong interferences from strong channel users. However, this issue is addressed by using SIC at the BS.

3) SIC at Receiver(s): In the downlink of a NOMA system, users with strong channels can achieve higher throughput gains by first decoding and canceling the messages of users with weaker channels before decoding their own signals. Conversely, in the uplink, to improve the throughput of users with weaker channels, the Base Station (BS) successively decodes and cancels the messages of users with strong channels before decoding the signals of users with weaker channels.
4) Inter-cell interference: In the downlink of a NOMA system, users in a cluster may experience additional interference from neighboring co-channel base stations (BSs). However, downlink inter-cell interference is similar to that of Orthogonal Multiple Access (OMA). For example, in a two-user NOMA cluster, interference from a neighboring co-channel BS is received by users due to the transmission power assigned to the neighboring BS. In OMA, the interference received by each user is comparable to NOMA, although it may differ for all users in the cluster. In the uplink NOMA, a larger number of users in neighboring co-channel BSs' NOMA clusters may result in more interference at the BS of interest. Hence, uplink multi-cell interference in NOMA is proportional to the number and transmission powers of users in neighboring co-channel BSs' NOMA clusters and is distinct from OMA.

2.5 The role of NOMA in Massive MIMO

To address the issue of spectrum scarcity in modern mobile networks caused by the exponential growth of mobile data traffic, non-orthogonal multiple access (NOMA) has emerged as a crucial multiple access (MA) technique. NOMA provides a promising solution by enabling multiple users to share the same time-frequency resources, leading to higher spectral efficiency and greater capacity in the same bandwidth. In this context, a new NOMA scheme is proposed for Massive MIMO systems that employs a superposition coding technique to transmit multiple signals to multiple users simultaneously. The proposed scheme also employs a limited feedback mechanism to estimate the channel state information (CSI) at the transmitter. This mechanism enables the transmitter to adjust the transmit power and codebooks based on the estimated CSI, resulting in improved system performance(Ding & Poor, 2016).

Orthogonal and superimposed pilot schemes are both effective in mitigating pilot contamination issues. However, the superimposed pilot scheme surpasses the orthogonal pilot scheme in terms of spectral efficiency and achievable rate. Although increasing the number of antennas can enhance the performance of both pilot schemes, the superimposed pilot scheme is more susceptible to the number of antennas. Additionally, the study emphasizes that having an excessive number of users can result in pilot contamination, leading to a decline in the performance of both pilot schemes (Ma et al., 2017).

It is important to note that conventional mMIMO methods, which utilize spatial multiplexing to provide service to multiple users on the same time/frequency/code resources and rely on beamforming to partially reduce inter-user interference, should not be considered as OMA (Orthogonal Multiple Access) techniques. In the HmNOMA technique, users are distinguished based on whether they would benefit from power-domain NOMA operation or not. Those that would benefit from power-domain NOMA are served using this technique, while those that would not are served using standard mMIMO. The combination of these methods results in better performance than using only NOMA or only mMIMO. However, when Non-Line-of-Sight (NLOS) scenarios are present, the improvement provided by HmNOMA is only moderate compared to using only mMIMO (Senel et al., 2019).

Non-orthogonal multiple access (NOMA) can enhance spectral efficiency in scenarios where the User Equipment (UEs) encounter unfavorable propagation conditions. For instance, this is true when the UEs are situated in close proximity to each other and the antenna array fails to provide sufficient resolution in the spatial domain(Le et al., 2019). The combination of Non-Orthogonal Multiple Access (NOMA) with Massive MIMO has the potential to enhance both the spectral efficiency (SE) through the application of NOMA, and the energy efficiency (EE) through the utilization of Massive MIMO. If perfect channel state information (CSI) is available and pilot contamination is completely eliminated, increasing the number of antennas will always result in a better system performance(Huang, 2020).

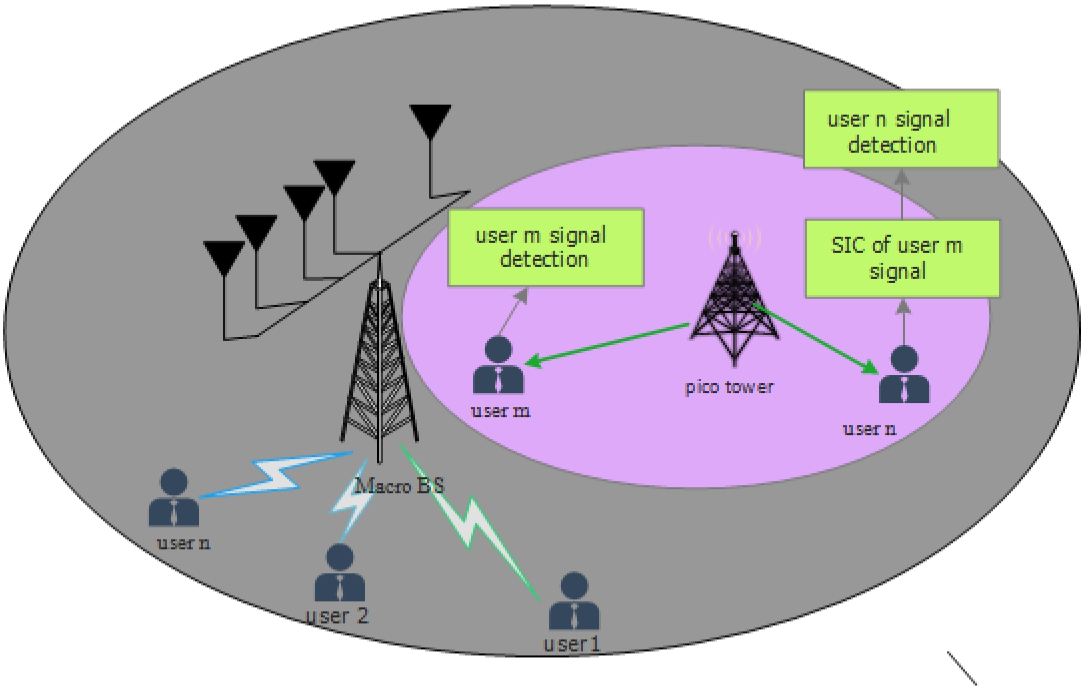

Figure 2.5: Illustration of NOMA and massive MIMO based hybrid HetNets (Y. Liu et al., n.d.)

Compared to HetNets based on orthogonal multiple access (OMA), Non-Orthogonal Multiple Access (NOMA) has the capability to improve the spectrum efficiency of the network. Macro cells augmented with Massive MIMO have the ability to provide increased array gain, which subsequently improves the average received power for the connected users. By increasing the bias factor, more users can be incentivized to connect to small cells, which is an effective approach to expanding the coverage of small cells or managing loading balance among different tiers of HetNets(Y. Liu et al., n.d.).

2.6 Rayleigh model

When the direct dominant path is not a line of sight channel between the transmitter and receiver (there is no correlation and no mutual coupling between the transmit antennas or the receiving antennas), Rayleigh fading is employed in the theoretical study of the massive MIMO system. Signal propagation in the ionospheric and troposphere is provided by this model. The Rayleigh distribution can be effectively employed to show the statistically time-varying character of the received spectrum in envelope of a flat fading signal or a single multipath component in mobile radio channels. The existence of numerous statistically independent reflected and scattered routes with random amplitudes that can be represented by an i.i.d. complex Gaussian random variable is one of the main assumptions of the Rayleigh model.

The envelope of the sum of two quadrature Gaussian noise signals conforms with a Rayleigh distribution. Then, the channel elements of Rayleigh fading channel is given by

$$h_{\text{Rayleigh}} = a + jb$$

where $a \sim \mathcal{N}\left(0,\frac{1}{2}\right)$, and $b \sim \mathcal{N}\left(0,\frac{1}{2}\right)$ are i.i.d. Gaussian random variable.

A Rayleigh fading channel is commonly used in wireless communication systems because it is a good model for the random variations in signal strength that occur due to multipath propagation. In a wireless communication system, signals transmitted from a transmitter can be received at a receiver through multiple paths, with each path having a different distance and reflection characteristics. This results in the received signal being a combination of multiple copies of the transmitted signal, each with a different amplitude and phase. The Rayleigh fading channel model assumes that the amplitudes and phases of the various signal components are randomly and independently distributed, which is a good approximation for many practical situations. The Rayleigh fading channel model is also computationally efficient and relatively easy to implement, making it a popular choice in wireless communication systems.

2.7 Related Works

In a system known as MIMO-NOMA, several users broadcast signals using the same time-frequency resources. Iterative receiver approaches, which incorporate numerous iterations of interference cancellation and decoding, are used to separate the signals at the receiver. The study uses linear precoding and decoding algorithms and makes the assumption that the receiver has perfect knowledge of the channel state information (CSI). Additionally, it evaluates how well the system performs in terms of error probability and rate that may be achieved under various operating circumstances, such as varying user and antenna numbers. The study also examines how various system characteristics, such as power distribution and iterations, affect performance. (Tominaga et al., 2022).

However, it does not investigate the impact of the number of antennas at the base station on the system performance. In a Massive MIMO system, the use of a large number of antennas at the base station can improve the system's spectral efficiency, energy efficiency, and interference management capabilities.

In wireless communication, precoding is a method that leverages the spatial diversity of multiple antennas to shape the transmitted signal and improve MIMO system performance. In contrast to previous research, a more practical scenario is considered, where the input signals are drawn from finite-alphabet constellation sets, such as phase shift keying (PSK) or quadrature amplitude modulation (QAM), instead of Gaussian signals(Zhu et al., 2019). Theoretical analysis and simulation results demonstrate that zero-forcing (ZF) and matched-filter (MF) precoders are nearly optimal when the base station (BS) has many more antennas than users, similar to the situation with Gaussian inputs. However, in practice, interference in massive MIMO systems can be more complicated and can considerably impact the effectiveness of linear precoding.

The relay-assisted NOMA system employs massive MIMO to improve system capacity performance. The non-regenerative massive MIMO-NOMA relay system is discussed in detail. The capacity and sum rate performances are positively correlated with the transmitter antenna, averaged power value, and number of users, while the performance is negatively correlated with the relay number. Compared to conventional MIMO-NOMA, relay-assisted NOMA, and massive MIMO orthogonal multiple access (OMA) schemes, the combined massive MIMO-NOMA scheme can achieve higher capacity performance(Zhang et al., 2017). When using non-regenerative relay systems, the signal received at the relay node may be affected by noise and interference, and the relay node itself can add more noise and distortion to the signal. The analysis being discussed only considers one particular receiver, which is (MMSE_SIC) receiver.

MIMO-NOMA is a combination of Multiple-Input Multiple-Output (MIMO) and Non-Orthogonal Multiple Access (NOMA) techniques. This combination can effectively address a range of heterogeneous challenges, such as massive connectivity, low latency, and high reliability(Chi et al., 2018). The article introduces a coded MIMO-NOMA system that can achieve near-capacity performance while maintaining low implementation complexity. To achieve this, the system uses a receiver that includes a multi-user Linear Minimum Mean-Square Error (LMMSE) detector and a bank of single-user message-passing decoders. These decoders divide the signal recovery process into simpler calculations that are performed separately. Additionally, the article proposes an asymptotic extrinsic information transfer analysis that can be used to estimate the performance of the iterative receiver. In this analysis, practical channel codes are developed to match the LMMSE detector in the iterative decoding perspective. However, in the upcoming generation, the proposed practical MIMO-NOMA system may not meet the capacity and spectral efficiency requirements. This is because practical MIMO-NOMA systems may not provide as much spatial diversity as massive MIMO-NOMA due to the smaller number of antennas used in the system. The achievable capacity and spectral efficiency of practical MIMO-NOMA systems may be limited due to the smaller number of antennas used in the system. As the number of users increases, interference between users in practical MIMO-NOMA may become more pronounced, leading to degraded system performance. In contrast, massive MIMO-NOMA can leverage a large number of antennas to mitigate interference and enhance system performance.

The article obtains closed-form expressions for lower bounds on the ergodic achievable rates of MRT and ZF precoding. For RZF precoding, the ergodic achievable rate is derived when the number of transmit antennas and users are large, but their ratio remains fixed. The proposed cache-aided massive MIMO scheme achieves much higher ergodic rates compared to conventional massive MIMO, particularly when the number of users approaches the number of transmit antennas. The performance gains achieved by the proposed scheme would not be possible if caching and massive MIMO were designed separately. Thus, the joint design of caching and massive MIMO, with interference cancellation and precoding optimization, is a promising approach to improve the spectral efficiency and energy efficiency of wireless communication systems(Wei et al., 2019). However, the use of cache memory introduces additional complexity in managing the cache contents and ensuring cache consistency, which may require additional overhead and complexity in the system design. Moreover, the performance gains achieved by the scheme may depend on the availability and relevance of cached data, which may be difficult to predict and manage effectively. These factors may limit the practical feasibility and scalability of the cache-aided massive MIMO approach in real-world wireless communication systems. It does not incorporate NOMA technology, which can further enhance the spectral efficiency and capacity of wireless communication systems by allowing multiple users to share the same time-frequency resources.

L-MUD design uses linear/nonlinear multi-user MIMO techniques for each MU-MIMO group, and a successive interference cancellation process for the NOMA layers. The new L-MUD design achieves complexity reductions, which can lead to significant power savings and extend the state-of-the-art of MIMO-NOMA towards green applications for 5G wireless networks and beyond. The designs that are presented enable effective use of the available spectrum while maintaining high levels of user connectivity, reliability, and power efficiency, which contributes to more towards green communication systems. (Al-Hussaibi & Ali, 2019). Nevertheless, reducing the transmission power of wireless devices can save energy, but it may also degrade the quality of service in terms of coverage, data rate, and reliability. Implementing GWN may require additional hardware and software components, such as energy harvesting devices, power management systems, and optimization algorithms, which can increase the cost of wireless communication systems.

In (Shi et al., 2022), the effectiveness of Multiple-input MIMO-NOMA systems with randomly placed users are investigated. The users are assumed to be randomly distributed according to a Poisson point process (PPP), and the Kronecker model which is used to model the spatial correlation between MIMO channels, while the composite channel model is used to capture both large-scale and small-scale fading. Prior studies on MIMO-NOMA systems have not accounted for the impact of the spatial randomness of user distribution, spatial correlation among antennas, and large-scale fading, making their analysis a challenging task. The article derives precise expressions for both the average outage probability and the average good put using ZF detection. Moreover, asymptotic analyses are conducted for both high and low signal-to-noise ratio (SNR) or small and large cell radius to provide more insightful results.

Table 2.1: Summary of related works

Title	Contribution	Limitation	Gap fulfilled
Performance Analysis of MIMO-NOMA Iterative Receivers for Massive Connectivity(Tominaga et al., 2022)	It analyzes the performance of the system in terms of the error probability and the achievable rate under	It doesn’t consider the use of a large number of antennas at the base station which can improve the system's spectral efficiency, energy	Considers the case massive antenna and takes into consideration the systems spectral efficiency.

	different operating conditions, such as varying number of users and antennas.	efficiency, and interference management capabilities.	
Performance Analysis of Linear Precoding in Massive MIMO Systems With Finite-Alphabet Inputs(Zhu et al., 2019).	A more realistic scenario, where the input signals are taken from finite-alphabet constellation sets, such as phase shift keying (PSK) or quadrature amplitude modulation (QAM), instead of Gaussian signals are considered.	ZF and MF precoders are near optimal when the number of antennas equipped at the BS is much larger than the number of users, which is similar to the case of Gaussian inputs.	Provides a detailed analysis of the performance of linear receivers in MIMO-NOMA systems for massive connectivity, considers the impact of imperfect channel estimation.
Practical MIMO-NOMA: Low Complexity and Capacity-Approaching Solution(Chi et al., 2018).	Address heterogeneous challenges, such as massive connectivity, low latency, and high reliability.	Practical MIMO-NOMA may not provide as much spatial diversity as massive MIMO-NOMA due to the smaller number of antennas used in the system.	Addresses spatial diversity of massive MIMO-NOMA

CHAPTER THREE

3. METHODS AND MATERIALS

3.1 Introduction

In this thesis, secondary sources of information related to linear receiver approaches for uplink massive MIMO NOMA systems were studied. These sources included journals, papers from the Institute of Electrical and Electronics Engineers (IEEE), and works by previous researchers. In large MIMO uplink systems, researchers used their own suggested methodologies to produce high-performing and simple transmitted signal detecting methods. Based on inputs from a review of related literature, a problem definition, and consideration of the analysis of various linear receiver's algorithms, the methodology of this work is illustrated as follows.

3.2 Materials

In this thesis study, programs like MATLAB/R2022b and Concept Draw DIAGRAM are employed. Using the computer language MATLAB, scientists and engineers can design and build systems and technologies that will change the world. The drawing program Concept Draw DIAGRAM comes with a complete set of professional drawing tools, ready-to-use templates, a substantial object library, and a number of custom printing and file export options.

3.3 Methods

3.3.1 Mathematical model of linear receiver's algorithms for massive MIMO NOMA

Working principle of linear receivers in uplink massive MIMO NOMA

Massive MIMO NOMA (Non-Orthogonal Multiple Access) with linear receivers is a communication system that enables multiple users to share the same frequency band by utilizing non-orthogonal signaling and linear receivers. The performance of this system can be analyzed by considering the following steps:

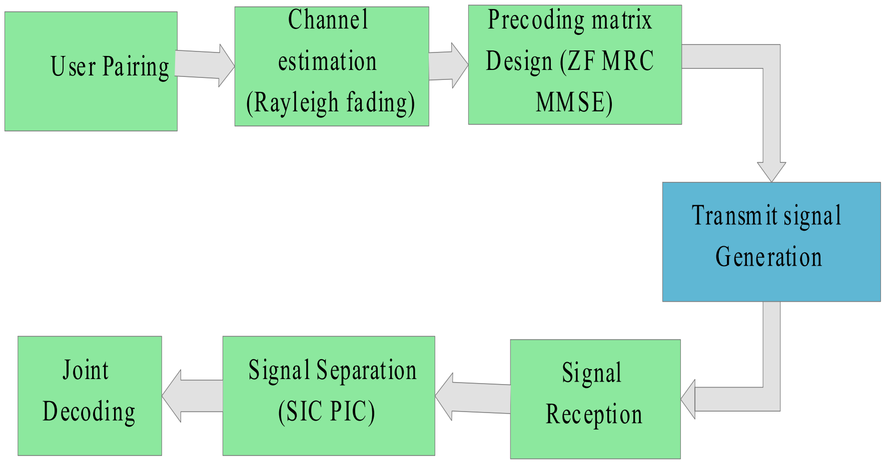

Figure 3. 1: working principle of massive MIMO NOMA

User Pairing: User pairing is the process of pairing multiple users together to form a cluster. In NOMA, multiple users can share the same time-frequency resources by using superposition coding. The pairing of users should be done in such a way that the users with better channel conditions are paired with weaker users to achieve better performance.

Channel Estimation: Channel estimation involves estimating the channel state information (CSI) between the base station and the users. In massive MIMO systems, the number of antennas at the base station is much larger than the number of users, which makes channel estimation more accurate. The estimated CSI is used to design the precoding matrix.

Precoding Matrix Design: Precoding is a technique used to enhance the signal quality by pre-multiplying the data symbols with a matrix that optimally combines the signals from multiple antennas. In massive MIMO systems, the precoding matrix is designed using the estimated CSI to maximize the signal quality and minimize the interference between users.

Transmit Signal Generation: After designing the precoding matrix, the base station generates a signal that is sent to the users. The signal is generated by multiplying the precoding matrix with the data symbols of each user and adding them together.

Signal Reception: The users receive the signal transmitted by the base station. The received signal is affected by noise, interference, and fading. The received signal is then processed by the linear receiver.

Signal Separation: In NOMA, the received signal contains superimposed signals from multiple users. To separate the signals from different users, the linear receiver applies a signal separation technique that utilizes the non-orthogonal nature of NOMA. The signal separation technique can be based on successive interference cancellation (SIC) or maximum likelihood (ML) decoding.

Joint Decoding: After separating the signals from different users, the linear receiver performs joint decoding to decode the data symbols of each user. Joint decoding involves decoding the data symbols of all users simultaneously by taking into account the interference between them.

Notation: lowercase bold face letters denote column vectors, while boldface upper case letters denote matrices. a_i is the i-th element of the column vector a, while A_i is the i-th row of the matrix A. $[A]_{ij}$ is the i-th row, j-th column element of the matrix $A. I_M$ is the identity matrix with size $M \times M$. The superscripts $(\cdot)^T$ and $(\cdot)^H$ denote the transpose and the conjugate transpose operators, respectively. The magnitude of a scalar quantity or the cardinality of a set is denoted by $|\cdot|$. The Euclidean norm of a vector is denoted by $\|\cdot\|$. The circularly symmetric complex Gaussian distribution with mean a and covariance **B** is denoted by $\mathcal{CN}(\mathbf{a}, \mathbf{B})$. E (), is the expectation of matrix.

3.4 System model

This study considers the case of a massive MIMO system with N antennas serving a number of K User Equipments (UEs). In conventional massive MIMO systems, each BS independently manages its own resources. The assumption taken is that neighboring receivers and their corresponding served devices are sufficiently distant from each other or are located in different indoor locations, and/or they transmit on different radio resource blocks, leading to negligible interference between them. In a single frequency channel, the K devices share the same radio resource in the form of a one-time slot. We presume that the channel undergoes Rayleigh fading, and the coherence time interval is longer than the duration of the time slot. Additionally, we assume that there may be more active devices in a given time slot than the number of antennas N at the receiver, i.e., K > N.

We consider a scenario where K single user devices transmit independent packets and are randomly distributed around a common massive antenna receiver as illustrated in Fig 3.2. We assume that nearby receivers and their corresponding served devices are sufficiently separated from one another (or at distinct indoor locations), and/or that they transmit on different radio resource blocks, so that the interference they cause to one another is insignificant.

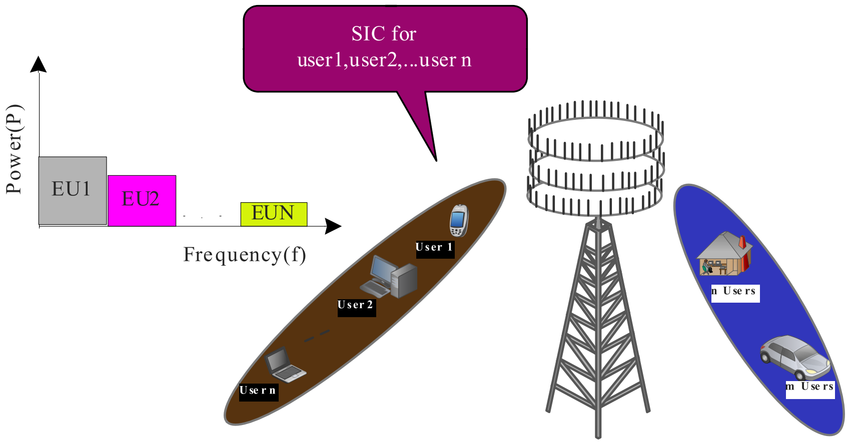

Figure 3. 2: System model of massive MIMO NOMA

When devices send packets, the packets are composed of two parts. The first part is the pilot sequence, which is used for channel estimation and activity detection. The second part is the payload, which contains the actual data being transmitted. It is assumed that the length of the pilot sequence is equal to or greater than the number of devices, which allows each device to be assigned a unique and orthogonal pilot sequence. The $N \times 1$ baseband received signal vector is given by

$$y = GP^{1/2}x + w \tag{1}$$

where $P \in \mathbb{R}^{K\times K}$ is a diagonal matrix containing the average transmit SNRs of the K MTC devices, $[P]_{kk} = p_k, G \in \mathbb{C}^{N\times K}$ is the matrix of channel gains between the K devices and the BS, $x \in \mathbb{C}^{K\times 1}$ is the vector of simultaneously transmitted symbols by the K devices, and $w \in \mathbb{C}^{N\times 1}$ is the vector of Additive White Gaussian Noise (AWGN) samples at the BS, such that $w \sim \mathcal{CN}(0_{N\times 1}, I_N)$ (that is, we assume that the noise power is normalized to one). Following the Shannon capacity framework, the symbols $\sqrt{p_k}x_k$ transmitted by the k^{th} MTC device follow a Gaussian distribution with variance p_k.

3.5 Channel Model

The wireless channel gain from the k-th device to the n-th receive antenna can be calculated using the n-row k column element of G as $g_{nk} = \sqrt{\beta_k}h_{nk}$, where $\beta_k < 1$ corresponds to the power attenuation due to distance, and the wireless channel coefficient h_{nk} is independent and identically distributed (i.i.d.), following a complex Gaussian distribution with zero mean and unit variance, i.e., $h_{nk} \sim \mathcal{CN}(0,1)$. Thus, the matrix of channel gains is

$$G = HB^{1/2} \tag{2}$$

where H is the $N \times K$ matrix of wireless channel coefficients between the K devices and the receiver antennas, with $[H]_{nk} = h_{nk}$, and B is a $K \times K$ diagonal matrix with $[B]_{kk} = \beta_k$.

We assume that the large-scale fading coefficients $\beta_k \forall k$ are known by the receiver. In order to avoid unnecessary power consumption and the near-far effect, the system adopts a channel inversion power control such that all devices have the same per antenna average received ρ (Goldsmith & Varaiya, 1997), thus

$$p_k = \rho\beta_k, \forall k \tag{3}$$

By considering the presence of channel estimation errors, the estimated $N \times K$ channel matrix between the K devices and the receiver can be rewritten as

$$\hat{G} = G - \tilde{G} \tag{4}$$

where $\tilde{G} \in \mathbb{C}^{N \times K}$ corresponds to the matrix of estimation errors, whose entries are i.i.d. and follow a complex Gaussian distribution with zero mean and variance σ_e^2, i.e., $[\tilde{G}]_{i,j} \sim \mathcal{CN}(0, \sigma_e^2)$. The receiver utilizes a Maximum Likelihood (ML) channel estimation algorithm, in which the channel estimates are obtained by using pilot sequences that are known to the receiver. In order to guarantee that all the pilot sequences are orthogonal to each other, their length must be at least equal to the number of served devices, i.e., $L \geq K$. The variance of the channel estimation errors associated to the channel estimates of the k-th device is (Eraslan et al., 2013),

$$\sigma_e^2 = \frac{1}{L\rho} \tag{5}$$

3.6 Linear Detection Schemes

3.6.1 Maximum-ratio combining

MRC is a very simple signal processing, where all the received signal elements are weighted and then combined to maximize the output SNR. Thus, in order to detect the transmitted signal from the k th user, the received signal y is multiplied by the conjugate-transpose of the channel vector g_k, according to the following expression (Albdran et al., 2017).

$$\hat{g}_k = \quad g_k^H y = \sqrt{p_u} \|g_k\|^2 x_k + \sqrt{p_u} \sum_{i=k}^{K} h_k^H g_i x_i + g_k^H n \tag{6}$$

where $\hat{g}_k$ is the estimated symbol of the k th user, p_u is the uplink data power, x_k is the transmitted symbol of the desired k th user, and x_i is the transmitted symbol of the interference ith user, where $(i = 1,2, \dots, K)$ and $i \neq k$. g_k is the channel vector of the desired k th user and h_i is the channel vector of the interference ith user. Note that Equation (6) consists of three terms: the first one is the desired signal of the k th user, the second term is the interference signal from other users, and the last term is the noise.

To get the theoretical upper bounds on channel capacity with MRC receiver, the received signal-to-interference-plus-noise ratio (SINR) of the k th user can be given by

$$\gamma_{\mathrm{mrc},k} = \frac{p_{\mathrm{s}} \|\mathbf{g}_k\|^4}{p_{\mathrm{i}} \sum_{i \neq k}^{K} |\mathbf{g}_k^B \mathbf{g}_i|^2 + \|\mathbf{g}_k\|^2} \tag{7}$$

The outage probability of MRC is given by:

$$\mathcal{P}_{\mathrm{out}} = 1 - \frac{\mathbb{E}\{D\}}{K} = \Pr\{\log_2(1 + \gamma_{\mathrm{mrc},k}) < R\} \tag{8}$$

where R is the target data rate in bits/s/Hz.

3.6.2 Zero-forcing (ZF) detection

Unlike the Maximum Ratio Combining (MRC) scheme, the ZF scheme has the ability to fully remove interference between users. With ZF detector, the received signal y is separated into K streams by multiplying it with $(\hat{G}^H \hat{G})^{-1} \hat{G}^H$ as follows (Albdran et al., 2017):

$$\hat{g} = (\hat{G}^H \hat{G})^{-1} \hat{G}^H \mathbf{y} = \sqrt{p_u} \mathbf{x} + (\hat{G}^H \hat{G})^{-1} \hat{G}^H \mathbf{n} \tag{9}$$

where $\hat{g}$ is the estimated vector of the transmitted signals from all users. The received SINR of the k th user is given by:

$$\gamma_{\mathrm{ZF},k} = \frac{p_u}{\left[(\hat{G}^H \hat{G})^{-1}\right]_{kk}} \tag{10}$$

One advantage of using ZF detection is that the signal processing involved is simple, and it works well in interference-limited scenarios. However, the performance of ZF detection can be impacted by noise enhancement because it ignores the effect of noise.

The outage probability of ZF is given by:

$$\mathcal{P}_{\text{out}} = 1 - \frac{\mathbb{E}\{D\}}{K} = \Pr\left\{\log_2\left(1 + \gamma_{\text{ZF},k}\right) < R\right\} \tag{11}$$

where R is the target data rate in bits/s/Hz.

3.6.3 Minimum mean-square error (MMSE) detection

In this subsection, the MMSE detection method is introduced. MMSE receiver maximizes the received SNR (Al Soufy et al., 2023). The received SINR for the MMSE receiver is expressed as:

$$SINR_{\text{mere },k} = p_2 \hat{g}_k^n \left(p_u \textstyle\sum_{i/k}^{K} \ \hat{g}_1 \hat{g}_i^{II} + \mathbf{I}_N\right)^{-1} \hat{g}_k \tag{12}$$

where $\mathbf{I}_N$ is the identity matrix.

The outage probability of MMSE is given by:

$$\mathcal{P}_{\text{out}} = 1 - \frac{\mathbb{E}\{D\}}{K} = \Pr\left\{\log_2\left(1 + \gamma_{\text{MMSE},k}\right) < R\right\} \tag{13}$$

where R is the target data rate in bits/s/Hz.

3.6.4 Linear receivers for Information Decoding

Let $\hat{A}$ be an $N \times K$ linear detector matrix at the receiver that is a function of the matrix of estimated channel gains $\hat{G}$, i.e., $\hat{A} = f(\hat{G})$. In (M. Liu et al., 2016), the authors studied the performance of three different linear decoders assuming perfect CSI: MRC, ZF and MMSE. The corresponding linear detector matrices considering imperfect CSI are

$$\hat{A}_{\text{MRC}} = \hat{G}, \tag{14}$$

$$\hat{A}_{\text{ZF}} = \hat{G}\left(\hat{G}^H \hat{G}\right)^{-1} \tag{15}$$

$$\hat{A}_{\text{MMSE}} = \left(\hat{G}\hat{G}^H + \frac{1}{\rho} I_N\right)^{-1} \hat{G} \tag{16}$$

Since (15) and (16) contain matrix inversions, the ZF and MMSE decoders are designed to be used only when the number of users, represented by the variable K, is less than or equal to the number of receive antennas, represented by the variable N. Therefore, in crowded Machine-Type Communication (mMTC) scenarios where the number of active devices may exceed the number of receive antennas, these decoders are not suitable. In contrast, the MRC decoder can be used regardless of the values of K and N, making it a more suitable option in such scenarios.

Then, the received signal after linear detection employing MRC, or ZF/MMSE when $K \leq N$, is split into K streams and given by

$$\begin{aligned} r &= \hat{A}^H y = \hat{A}^H P^{1/2}(\hat{G} + \tilde{G})x + \hat{A}^H w \\ &= \hat{A}^H P^{1/2}\hat{G}x + \hat{A}^H P^{1/2}\tilde{G}x + \hat{A}^H w. \end{aligned} \tag{17}$$

Let r_k and x_k denote the k-th element of the $K \times 1$ vectors r and x, respectively. The have

$$r_k = \sqrt{\rho}\hat{a}_k^H g_k x_k + \sqrt{\rho}\hat{a}_k^H \sum_{k' \neq k}^{K} \hat{g}_{k'} x_{k'} + \sqrt{\rho}\hat{a}_k^H \sum_{k'' \neq k}^{K} \tilde{g}_{k''} x_{k''} + \hat{a}_k^H w, \tag{18}$$

where $\hat{a}_k, g_k, \hat{g}_k$ and $\tilde{g}_k$ denote the k-th column of the matrices $\hat{A}, G, \hat{G}$ and $\tilde{G}$, respectively.

3.6.5 SIC and PIC Decoding

To enhance the performance of a system in the presence of multiple concurrently active devices, one can utilize non-orthogonal multiple access (NOMA) with either successive interference cancellation (SIC) or parallel interference cancellation (PIC) decoding techniques. In SIC decoding, the active devices are arranged in a predetermined order based on a certain criterion. The receiver then attempts to decode the transmission of one active device during each decoding step while treating the signals of other active devices as interference. If the decoding process is successful, the receiver eliminates the interference caused by that device from the received signal. On the other hand, the PIC decoding technique aims to decode and eliminate the signal contribution of multiple active devices simultaneously during a single decoding step.

Suppose we are at a particular stage of the decoding process where the decoding of the k-th device is in progress. Devices with indices $\{1, \dots, k-1\}$ have been decoded successfully, and their signal contribution has already been removed from the received signal. Nonetheless, due to imperfect channel state information (CSI), their signal contribution was subtracted based on their estimated channel vectors, rather than their actual values. Consequently, there remains residual interference from these devices on the composite received signal, which is dependent on the level of CSI errors. At this particular stage of the SIC decoding process, we have:

$$r_k = \sqrt{\rho}\hat{a}_k^H g_k x_k + \sqrt{\rho}\hat{a}_k^H \sum_{k'=k+1}^{K} g_{k'} x_{k'} + \sqrt{\rho}\hat{a}_k^H \sum_{k''=1}^{k-1} \tilde{g}_{k''} x_{k''} + \hat{a}_k^H w \tag{19}$$

The first summation corresponds to the interference of the devices waiting to be decoded, while the second summation corresponds to the residual interference from the devices that have been correctly decoded.

Note that the interference due to imperfect CSI is cumulative, i.e., it continuously increases during the SIC decoding procedure. The post-processing SINR at the receiver while decoding the signal from the k-th device, including the effect of imperfect CSI, is given by

$$\gamma_k = \frac{\rho|\hat{a}_k^H g_k|^2}{\rho \sum_{k'=k+1}^{K} |\hat{a}_k^H g_{k'}|^2 + \rho \sum_{k''=1}^{k-1} |\hat{a}_k^H \tilde{g}_{k''}| + \|\hat{a}_k^H\|^2} \tag{20}$$

The signal transmitted by the k-th device is correctly decoded if $\log_2(1+\gamma_k) \geq R$, where R is the target data rate in bits/s/Hz. The SIC decoding procedure ends after all the K devices have already been correctly decoded or if no devices are correctly decoded at a decoding step.

3.7 Linear receivers with SIC/PIC operations

The following techniques can be employed when K>N, or the number of devices exceeds the number of receive antenna elements.

3.7.1 MRC_SIC

There is a linear detector and successive interference cancellation in the actual receiver structure(S. Wang et al., 2017). MRC-SIC is a technique that uses multiple antennas at the receiver to capture signals from multiple users. The received signals from each antenna are combined using a method called maximal ratio-combining. This technique assigns weights to each signal based on its signal-to-noise ratio (SNR) and combines them to maximize the overall SNR. The result is a single combined signal that is used for further processing.

Once the individual signals are received, they are combined and processed using SIC technique to eliminate interference caused by signals from previously detected users. SIC is an iterative technique that estimates signals from the remaining users, cancels their interference, and detects their signals. The MRC-SIC detector is particularly advantageous in scenarios with many users and strong interference. It can improve system performance by reducing interference between users and enhancing detection accuracy. For the MRC-SIC detection, the processed received signal for the i-th user is expressed as

$$\tilde{\mathbf{y}}^{\mathrm{MRC-SIC}} = \hat{\mathbf{g}}_k^H \hat{\mathbf{g}}_k x_k + \sum_{j>k} \hat{\mathbf{g}}_k^H \hat{\mathbf{h}}_j x_j + \sum_{j} \hat{\mathbf{g}}_k^H \mathbf{e}_j x_j + \hat{\mathbf{g}}_k^H (\mathbf{w} + \mathbf{q}) \tag{21}$$

Where, $\hat{\mathbf{g}}_i$ is estimated channel vector for the i-th user, x_i the transmitted signal from the i-th user, w is the additive white Gaussian noise (AWGN) component of the received signal, q is the interference caused by other sources, such as co-channel interference or inter-symbol interference.

$\sum_{j>k} \hat{\mathbf{g}}_k^H \hat{\mathbf{h}}_j x_j$, is the interference caused by the signals from other users that have been detected and cancelled out by SIC.

$\sum_j \hat{\mathbf{h}}_i^H \mathbf{e}_j x_j$, the interference caused by the signals from other users that have not yet been detected and cancelled out by SIC, but may be estimated based on their channel vectors.

Thus, the SINR of the k-th user is given by the following:

$$\gamma_k^{\text{MRC-SIC}} = \frac{\|\hat{\mathbf{g}}_k\|^4}{\sum_{j>k} \left|\hat{\mathbf{g}}_k^H \mathrm{g}_j\right|^2 + \sum_j \left|\hat{\mathbf{g}}_k^H \mathbf{e}_j\right|^2 + \frac{\left(\sigma^2+\sigma_i^2\right)}{P}\|\hat{\mathbf{g}}_k\|^2} \tag{22}$$

Where,

$\sum_{j>k} \left|\hat{\mathbf{g}}_k^H \mathrm{g}_j\right|^2$, the interference caused by the signals from other users that have been detected and cancelled out by SIC.

$\sum_j \left|\hat{\mathbf{g}}_k^H \mathbf{e}_j\right|^2$, the interference caused by the signals from other users that have not yet been detected and cancelled out by SIC, but may be estimated based on their channel vectors.

σ^2, the power of the AWGN component of the received signal.

σ_i^2, the power of the interference caused by other sources, such asco-channel interference or inter-symbol interference, that is not accounted for by the SIC process.

P, the total power available for transmission by all users.

3.7.2 ZF-PIC and MMSE-PIC

The ZF-SIC and MMSE-SIC receivers can only handle decoding and subtracting one user's signal contribution during each iteration. This means that a new ZF or MMSE filter needs to be computed after each SIC operation, resulting in a significant amount of complex operations, such as matrix inversions. As the number of receive antennas increases, the complexity of these operations also increases exponentially.

In contrast, ZF-PIC and MMSE-PIC receivers require fewer complex signal operations, such as matrix inversions, and can be used even when the number of users (K) is greater than the number of receive antennas (N). Multiple users can be decoded simultaneously at each decoding step, significantly reducing the number of ZF/MMSE operations required. Additionally, interference from all the correctly decoded devices is subtracted at the same decoding step, further reducing the computational complexity.

3.7.3 Computational Complexity of receivers

The objective of this section is to evaluate and compare the computational complexity of different receivers in a scenario where the transmitted signals of all K devices are decoded accurately in the long run. Initially, we provide an overview of the computational complexity involved in all the signal processing operations that the receivers are capable of performing:

- Arithmetic operations with individual elements has complexity O(1), thus each SIC operation has complexity O(N).
- Addition of two N × N matrices has complexity O(N × N) = O(N 2).
- The linear detection operation r = Ay is the product of a N × N matrix by a N × 1 vector, thus its complexity is O(N × N × 1) = O(N 2).
- The product of a N × M matrix by a M × P matrix has complexity O(N × M × P), thus each matrix multiplication required by the ZF or MMSE operations has complexity O(N 3).
- Matrix inversion has complexity O(N 3).

In asymptotic case of K = N, it is assumed that all signals transmitted by the K devices are decoded successfully in the first zero-forcing (ZF) or minimum mean square error (MMSE) operation, thereby eliminating the need for a post-interference cancellation (PIC) operation. The MRC-SIC scheme does not require any matrix inversion, but due to the increased number of iterations, its computational complexity is comparable to receivers that utilize matrix inversions. However, for K > N, the proposed ZF-PIC and MMSE-PIC receivers reduce the number of required matrix inversions as they can decode and subtract the signal contribution of multiple users in the same iteration.

In this study we will consider two parameters to measure the computational complexity of linear receivers:

3.7.3.1 Average number of matrix inversion

Performing matrix inversion is a time-consuming process, particularly for large matrices. In certain algorithms, such as those utilized in communication systems and signal processing, matrix inversion is frequently performed. As a result, the average number of matrix inversions can be utilized as a metric to assess the computational complexity of these algorithms. In this scenario, the linear receiver algorithm requires the calculation of the inverse of a significant matrix, which can be computationally demanding. The average number of matrix inversions is used to assess how frequently this operation is carried out on average during the execution of the linear receiver algorithm.

3.7.3.2 Average number of SIC operation

The average number of SIC operations is a metric that measures the computational complexity of wireless communication systems. SIC is a technique used in NOMA to separate signals from multiple users. Each SIC operation involves decoding one user's data symbols by eliminating interference from other users. The average number of SIC operations performed to separate all users' signals is a measure of computational complexity, as each SIC operation requires computation. The number of SIC operations needed depends on the number of users, channel conditions, and modulation scheme. Typically, the number of SIC operations increases with the number of users and decreases with better channel conditions and higher-order modulation schemes.

3.7.4 Performance metrics

3.7.4.1 Outage probability

Outage probability is a metric used to analyze the reliability of a communication system or network. It is defined as the probability that the system or network fails to meet a certain performance requirement, such as a minimum data rate or signal quality, during a given period of time. In wireless communications, outage probability is often used to characterize the probability that the quality of a wireless link falls below a certain threshold due to interference or fading. For example, in a cellular network, the outage probability may be defined as the probability that a user's signal-to-interference-plus-noise ratio (SINR) falls below a certain threshold, such as the minimum SINR required to maintain a certain data rate. Moreover, let D denote the number of correctly decoded signals at each time slot. Then, the outage probability is

$$\mathcal{P}_{\text{out}} = 1 - \frac{\mathbb{E}\{D\}}{K} = \Pr\{\log_2(1+\gamma_k) < R\} \tag{23}$$

3.7.4.2 Spectral Efficiency

Massive MIMO-NOMA with linear receivers can significantly improve the spectral efficiency of wireless communication systems by allowing multiple users to share the same resources through power allocation based on channel conditions. The spectral efficiency depends on factors such as the number of antennas, users, and modulation scheme. It can be higher than a conventional system due to the increased capacity enabled by the power allocation scheme and large number of antennas. However, the actual spectral efficiency depends on system parameters and implementation details.

The spectral efficiency formula for massive MIMO NOMA can be expressed as:

$$SE = (1/B) * \sum_{k=1}^{K} log_2(1 + \gamma_k) \quad (24)$$

where SE is the spectral efficiency in bits per second per Hertz (bps/Hz), B is the bandwidth in Hertz, K is the number of users in the system, γ_k is the SINR of the k^{th} user.

3.8 Proposed method

MMSE-SIC with QR decomposition is a proposed method for massive MIMO NOMA systems that can improve the performance of wireless communication networks. QR decomposition is a matrix factorization technique that decomposes a matrix into an orthogonal matrix and an upper triangular matrix. The QR decomposition can be used to reduce the computational complexity of MMSE-SIC in massive MIMO NOMA systems. In this proposed method, the received signals are first preprocessed using QR decomposition to obtain an orthogonal matrix Q and an upper triangular matrix R. The MMSE-SIC algorithm is then applied to the modified received signals using the QR decomposition. The QR decomposition reduces the computational complexity of MMSE-SIC by allowing the receiver to cancel the interference of multiple users efficiently, using the upper triangular matrix R. The orthogonal matrix Q can be used to detect the signals of each user separately.

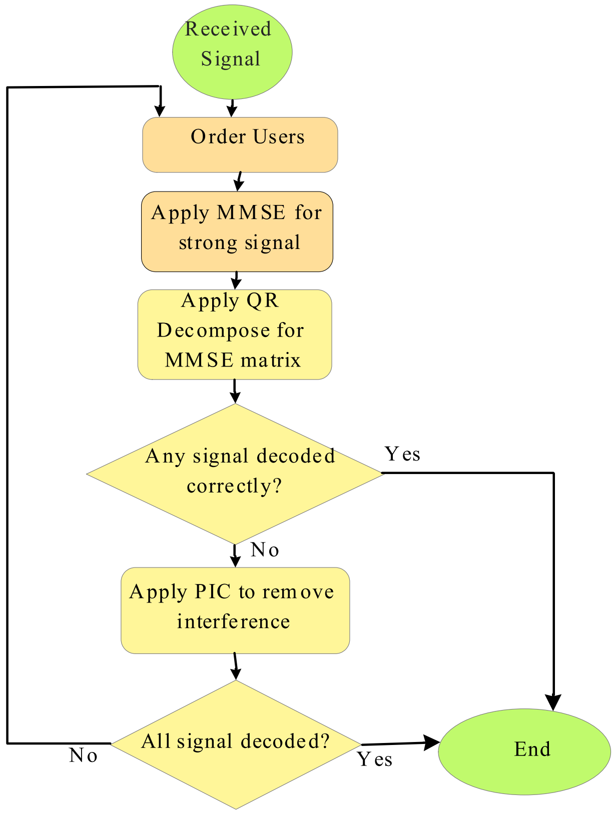

Figure 3. 3: Flow chart of the proposed method

The flowchart outlines the signal processing steps involved in decoding the received signal in a NOMA system with multiple ordered users. The first step involves ordering the users based on their channel strengths to identify the strong users that can be decoded first. The next step is to apply the MMSE technique to the signals from the strong users, which is used to estimate the transmitted signals and mitigate the effects of interference. QR decomposition is then applied to the MMSE matrix to simplify it and make it easier to remove interference. Finally, the PIC technique is used to remove interference from the weaker users by subtracting the decoded signals of the strong users from the received signal to obtain the residual signal.

CHAPTER FOUR

4. RESULTS AND DISCUSSIONS

This chapter is presenting the results of a simulation that was conducted to achieve a specific objective. The simulation focused on studying the performance of different linear receivers for massive MIMO NOMA (Non-Orthogonal Multiple Access) under a channel distribution called Rayleigh fading. The chapter includes a discussion of the simulation results and how different linear receivers performed under the Rayleigh distribution channel. The complexity of the linear receivers was also analyzed and discussed as the number of antennas and users increased. The simulation parameters used in this thesis work to evaluate the performance and complexity of analysis of different linear receivers for uplink massive MIMO NOMA are listed in the table.

Table 4.1: Simulation parameters

No	Simulation parameters	Type and value
1	Channel	Rayleigh fading
2	Linear receivers	ZF,MRC,MMSE
3	Noise	AWGN
4	SNR	Normalized
5	Length of the pilot sequence	K
6	Number of antenna(N)	64,128
7	Number of user(K)	64,128
8	Data rate(R)	0.5,1
9	Number of Monte Carlo runs(MC)	1e4, 1e5
10	Bandwidth(B)	1e6

N.B: For a plot that shows results obtained using both perfect and imperfect CSI, the line with dots represents the imperfect channel CSI. On the other hand, the smooth line represents the results obtained using perfect CSI.

4.1 Performance Analysis of Different Linear Receivers for Massive MIMO NOMA

4.1.1 Performance Comparison of Linear Receivers Based on Outage Probability

The linear receivers and combined receivers considered in the figure 4.1 are maximum ratio combining (MRC), MRC with successive interference cancellation (MRC-SIC), zero-forcing (ZF), minimum mean-squared error (MMSE), ZF with parallel interference cancellation (ZF-PIC), and MMSE with PIC (MMSE-PIC). The CSI assumptions considered are perfect CSI and imperfect CSI. The value of K and N are equal which is K=N=64. As we can see from the graph perfect CSI receivers have a good performance than imperfect CSI. In both cases MMSE_PIC has a best performance than others. Whereas, MRC has a less performance than other receivers.

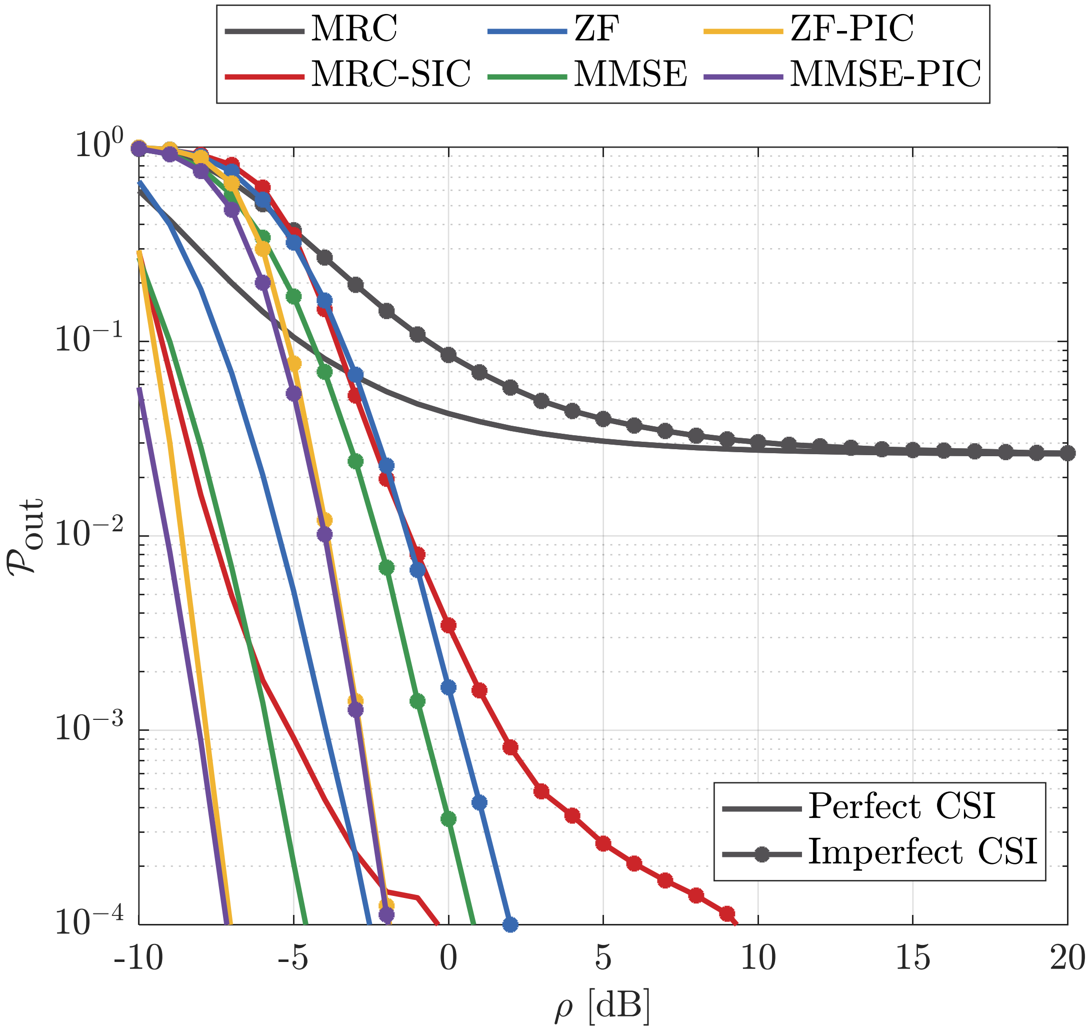

Figure 4. 1: Outage probability versus SNR when N=K=64, r=1

For any linear receiver, the outage probability is low when perfect CSI is available, while it is high when the CSI is imperfect. This is because in the case of perfect CSI, the receiver has access to accurate information about the wireless channel, which allows it to design an optimal receiver that reduces the likelihood of errors. By utilizing this channel information, the receiver can select the most appropriate parameters, such as the equalizer coefficients, that maximize the received signal power and minimize any interference and noise.

Consequently, the outage probability is low because the receiver can effectively compensate for any channel distortions.

4.1.2 Complexity measurement

The average number of matrix inversions and iterative SIC operations can be used as metrics to compare the complexity of different receiver algorithms, or to evaluate the performance of the same algorithm under different system conditions. For SNR greater than zero, $\rho > 0$ all linear recievers have constant average number of matrix inversion which is 1 except that MRC_SIC which is zero at any condition as it is shown in figure 4.2. ZF-PIC and MMSE-PIC have different values of average number of matrix inversion for $\rho < 0$. This is because, at lower values of ρ, the ZF-PIC and MMSE-PIC receivers require more iterations to decode the signals transmitted by K users. As the value of ρ increases, all K signals can be successfully decoded in a single iteration.

In the case of imperfect CSI at low SNR, ZF_PIC and MMSE_PIC has high average number of matrix inversion. The ZF receiver tries to eliminate the interference by inverting the channel matrix, which can be computationally intensive. Similarly, the MMSE receiver also requires the inversion of the channel matrix, which can be very complex at low SNR.

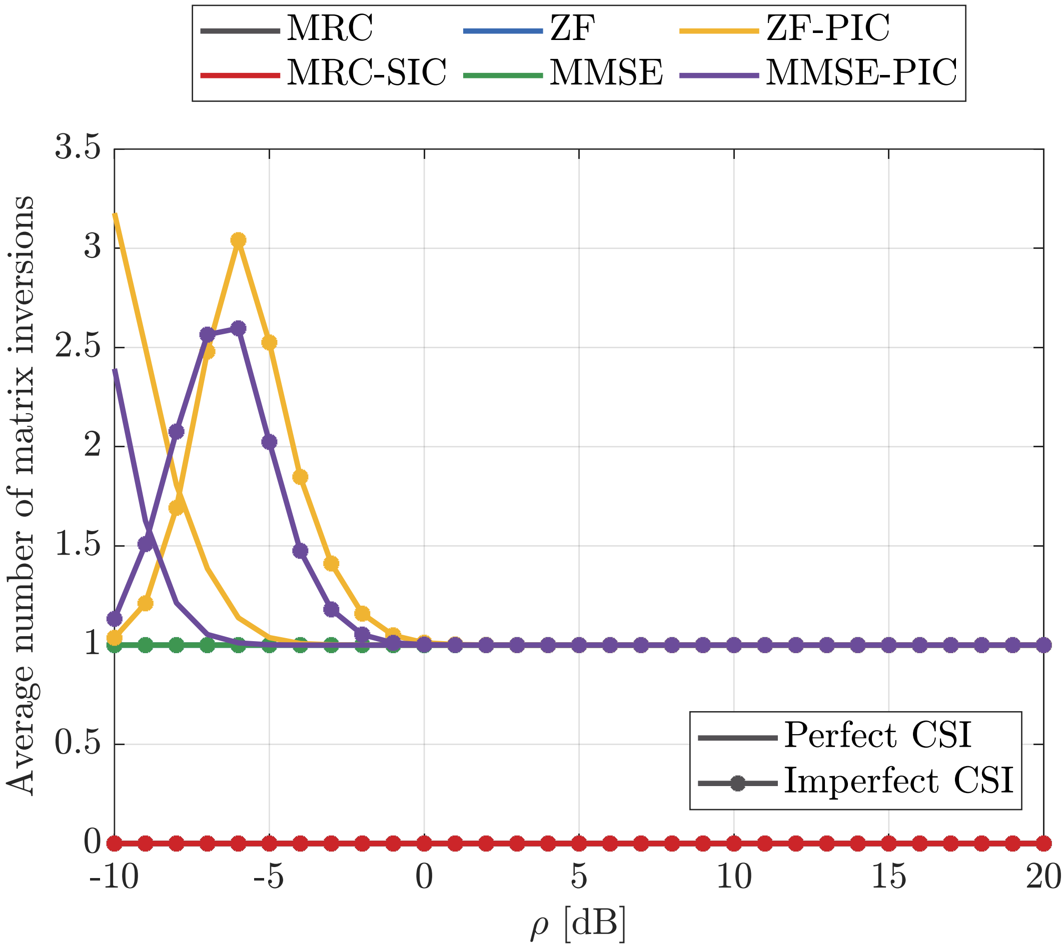

Figure 4. 2: Average number of matrix inversion versus SNR with N=K=64

The ZF-PIC (parallel interference cancellation) and MMSE-PIC receivers are iterative versions of the ZF and MMSE receivers, respectively, that use the interference cancellation technique to improve their performance. However, at low SNR($\rho < -6$), these receivers still require a large number of matrix inversions to accurately estimate the channel and at $\rho > -5$ it starts to decrease. As a result, the average number of matrix inversions is high for these receivers with imperfect CSI.

The MRC, ZF, and MMSE receivers are not designed to perform any SIC (Successive Interference Cancellation) operation. As we can see from the result of figure 4.3 the MRC-SIC, ZF-SIC, and MMSE-PIC remain constant after a certain value of ρ, typically when ρ is greater than zero. However, when ρ is less than zero, the average number of SIC operations required by the MRC-SIC algorithm increases with higher SNR values.

The average number of SIC operation for ZF_PIC and MMSE_PIC in the case of imperfect CSI is high, because these receivers need to perform a large number of SIC operations to remove the interference caused by other users. With imperfect CSI, the receiver not be able to accurately estimate the interference levels and need to perform multiple iterations of SIC to remove the interference. At low SNR, ($\rho > -4$) for ZF_PIC and ($\rho > -6$) for MMSE_PIC, the average number of SIC operation increases.

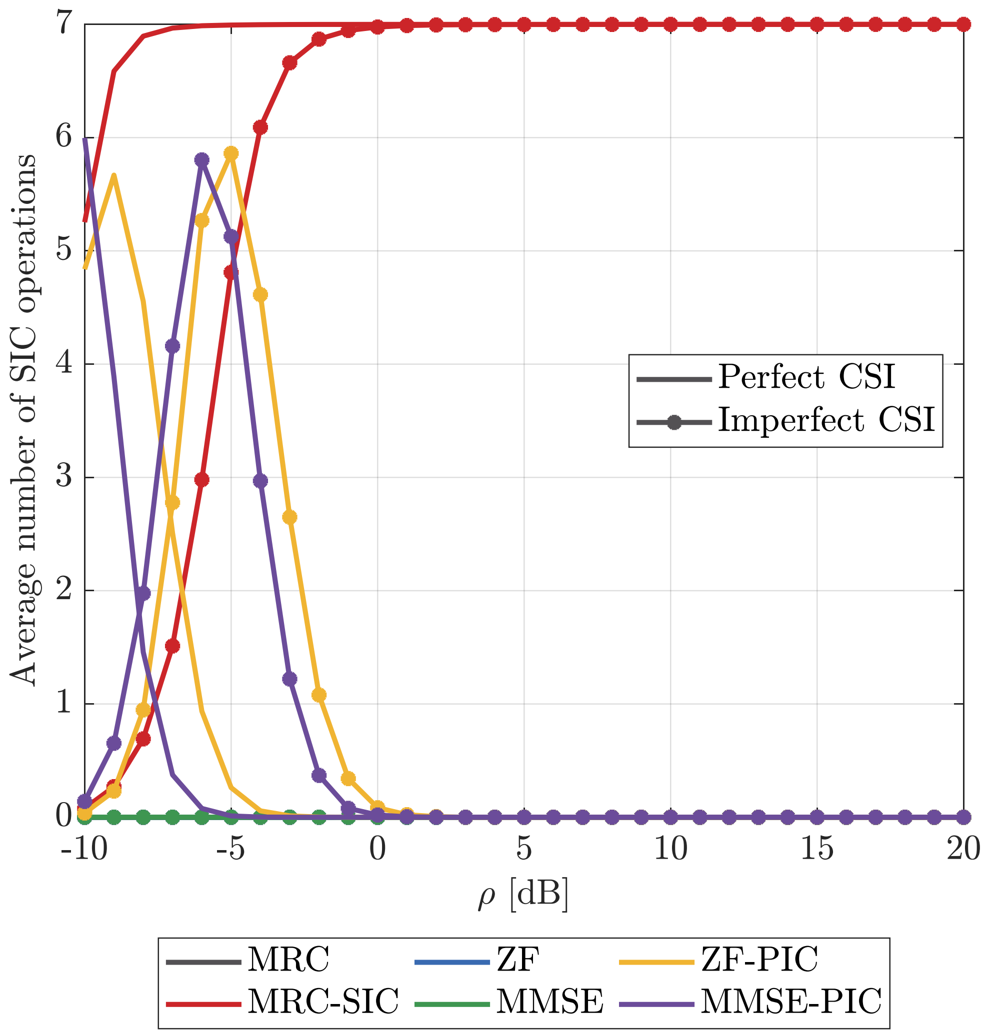

Figure 4.3: Average number of SIC operation versus SNR with N=K=64

As the number of antennas increases in massive MIMO systems, the outage probability can decrease, indicating better performance. However, increasing the number of antennas also increases the computational complexity of the system.

Despite this trade-off, it has been observed in figure 4.4 that at k=N=128, MMSE with parallel interference cancellation (MMSE-PIC) is the best performing parameter, while maximum ratio combining (MRC) is the least performing parameter in both scenarios of perfect and imperfect channel state information (CSI). This indicates that MMSE-PIC can provide better performance at higher numbers of antennas, while MRC may not be as effective.

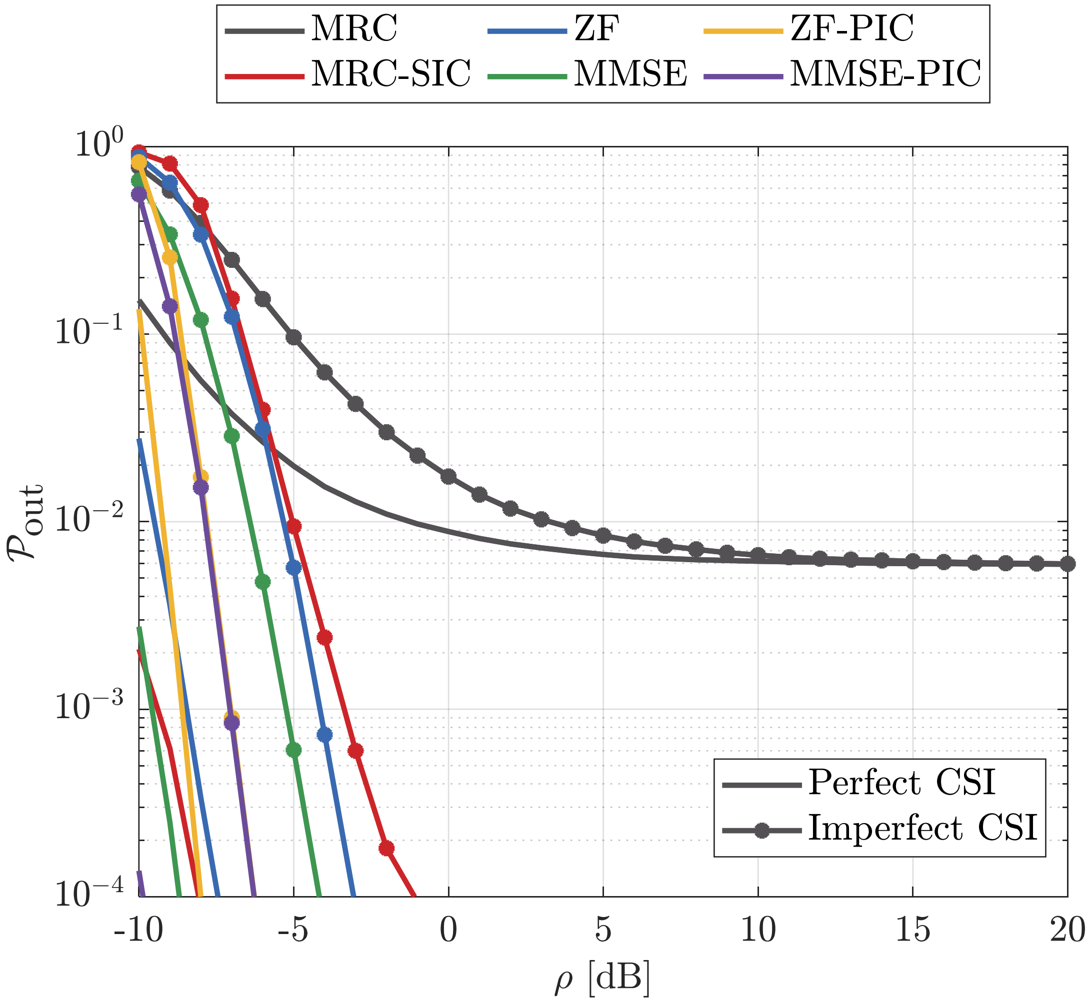

Figure 4. 4: Outage probability versus SNR when N=K=128, r=1

The MMSE_PIC which is the one has less outage probability in the case of N=K=64, has much less outage probability than the first one. The same goes for the others too. In the case perfect CSI, MMSE_PIC has 0.0001 outage probability when SNR is -10 which is very small. Therefore, as number of antenna increase with SNR the outage probability decreases.

As the number of antennas increases in massive MIMO systems, the computational complexity of linear receivers can be reduced rapidly, resulting in fewer matrix inversions on average as the signal-to-noise ratio (SNR) increases. This can be observed in the figure 4.5, where the average number of matrix inversions decreases as the SNR value increases. The average number of matrix inversions for maximum ratio combining (MRC) and MRC-SIC is zero for any value of SNR. However, for ZF and MMSE linear receivers, the average number of matrix inversions is constant and equal to one. In the case of imperfect channel state information (CSI), the average number of matrix inversions for ZF with ZF-PIC and MMSE with MMSE-PIC becomes constant at one for values of ρ greater than 0.6. therefore, since the one which has a high average number of matrix inversion is the complex one.

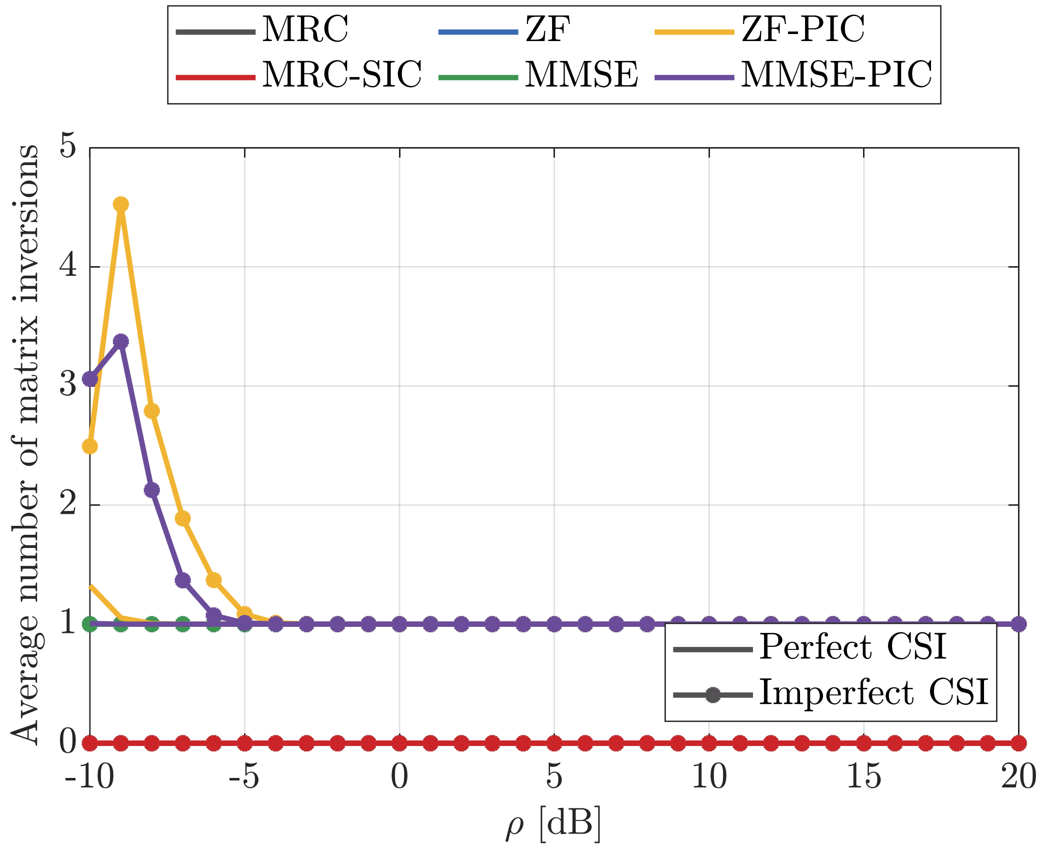

Figure 4. 5: Average number of matrix inversion versus SNR with N=K=128, r=1

It is apparent that the maximum value of the average matrix inversion for perfect and imperfect ZF_PIC is 1.3877 and 4.525, respectively. Although the imperfect value is initially higher, it quickly drops to one. Generally, when the number of antennas increases, the complexity decreases in case of the average number of matrix inversions.

The figure 4.6 shows that the average number of SIC operations for perfect channel state information (CSI) is constant for each linear receiver. It can be observed that all receivers have an average number of zero SIC operations, except for MRC-SIC, which has an average number of highest SIC operations and ZF-PIC which has decreasing value at first.

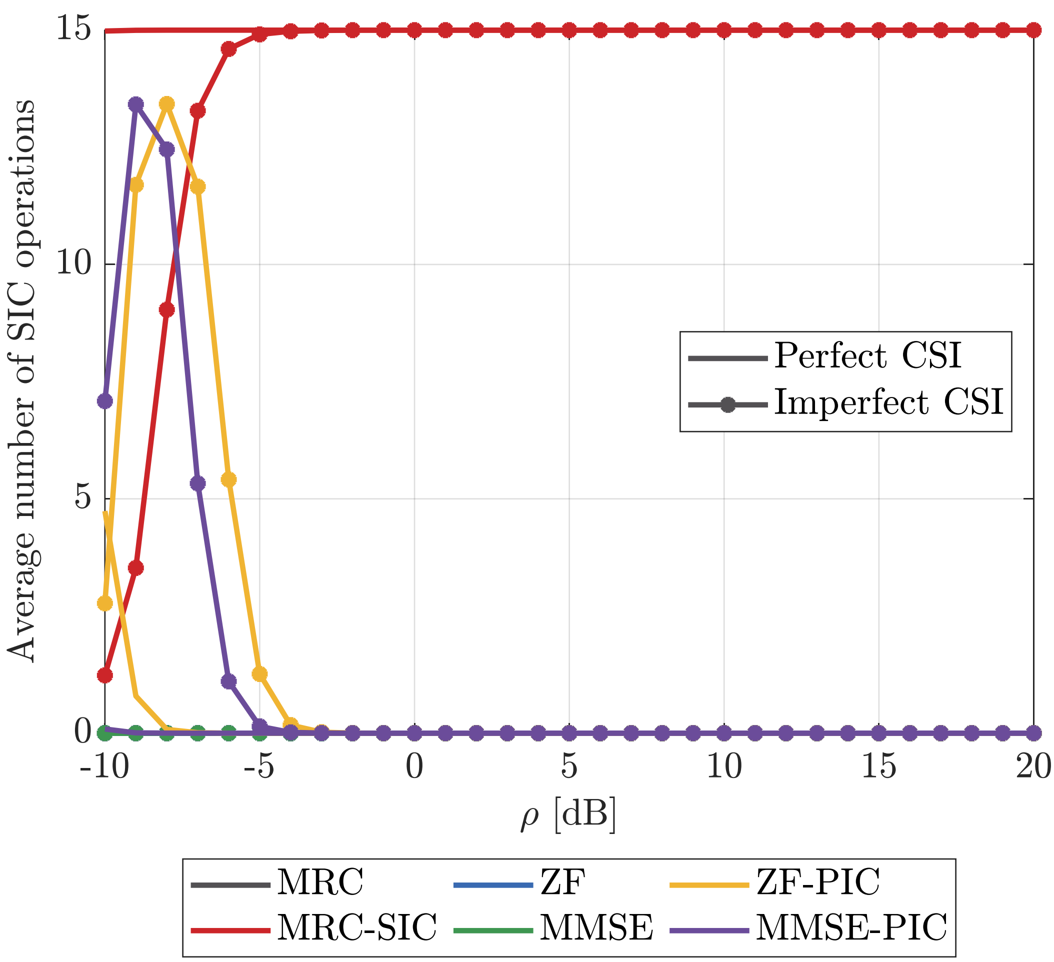

Figure 4. 6:Average number of SIC operation with N=K=128, r=1

Since ZF, MRC and MMSE no(zero) SIC operation taken pace their complexity is less. But, MRC case combined with SIC technique the result is vice versa. MRC_SIC, is the only receiver that has higher SIC operation for both perfect and imperfect CSI case.

Other receivers have less average number of SIC operation for the case of perfect CSI. For the case of MMSE_PIC, the average number of SIC operation is zero from the beginning for perfect CSI. Therefore, we can observe that except for that of MRC_SIC, other receivers which are combined with that of PIC operations have less complexity as number of antenna increase in the case of average number of SIC operation.

4.1.3 Spectral efficiency

Massive MIMO-NOMA with linear receivers can significantly improve the spectral efficiency of wireless communication systems by allowing multiple users to share the same resources through power allocation based on channel conditions. The spectral efficiency depends on factors such as the number of antennas, users, and modulation scheme. It can be higher than a conventional system due to the increased capacity enabled by the power allocation scheme and large number of antennas. However, the actual spectral efficiency depends on system parameters and implementation details. In this section we will see the spectral efficiency in the condition where K=N=128 for both perfect and imperfect channel estimation.

Based on Figure 4.7, it is evident that the spectral efficiency of perfect MMSE_PIC outperforms other receivers and has a consistently high level of performance. On the other hand, the maximum ratio combining (MRC) method has a much lower value of spectral efficiency. At low SNR values, the received signal at less value of SNR overwhelmed by noise, resulting in errors in the received data. The zero-forcing (ZF) equalizer used in the ZF_PIC receiver attempts to remove the effects of channel distortion, but it may not be able to completely eliminate the noise. This can lead to instability in the spectral efficiency graph as the performance of the ZF_PIC receiver becomes more sensitive to variations in the SNR.

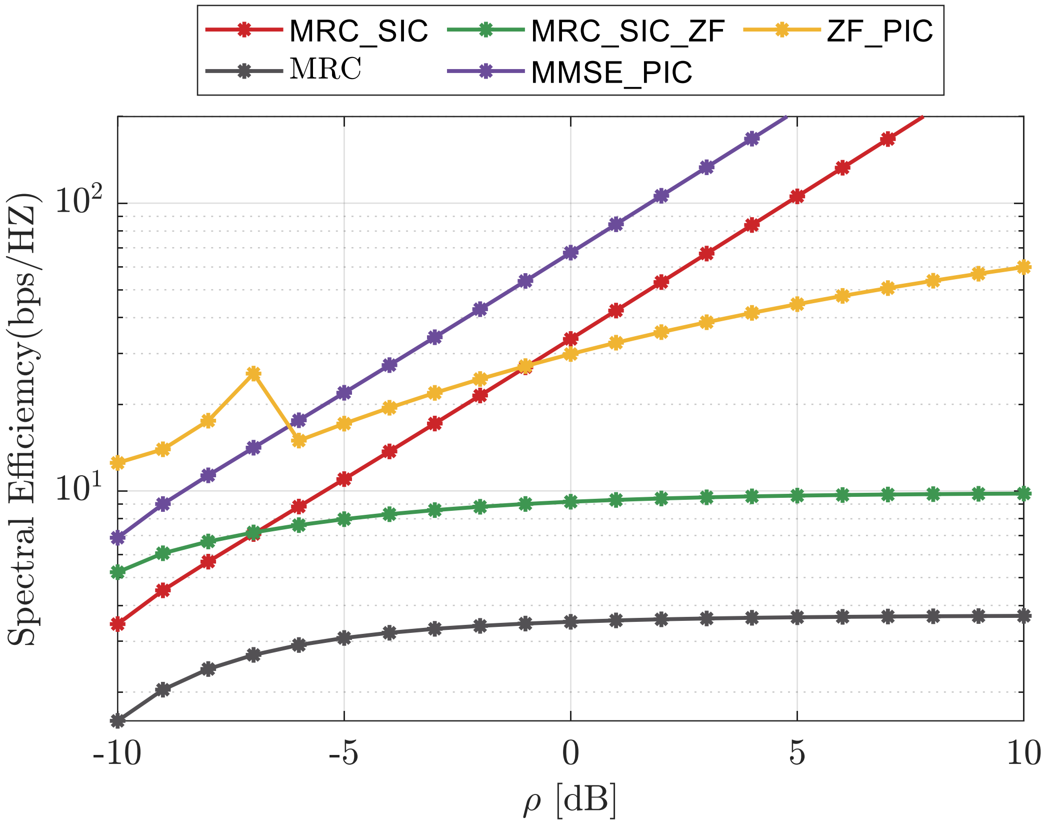

Figure 4.7: Spectral efficiency where K=N=128 in perfect CSI.

In figure 4.8, at low to moderate signal-to-noise ratio (SNR), the impact of the errors in CSI estimation is more significant, and the performance of the receiver is more sensitive to variations in the estimated channel. As a result, the initial portion of the spectral efficiency graph with imperfect CSI may be unstable, as the receiver struggles to accurately estimate the channel and adjust its processing accordingly.

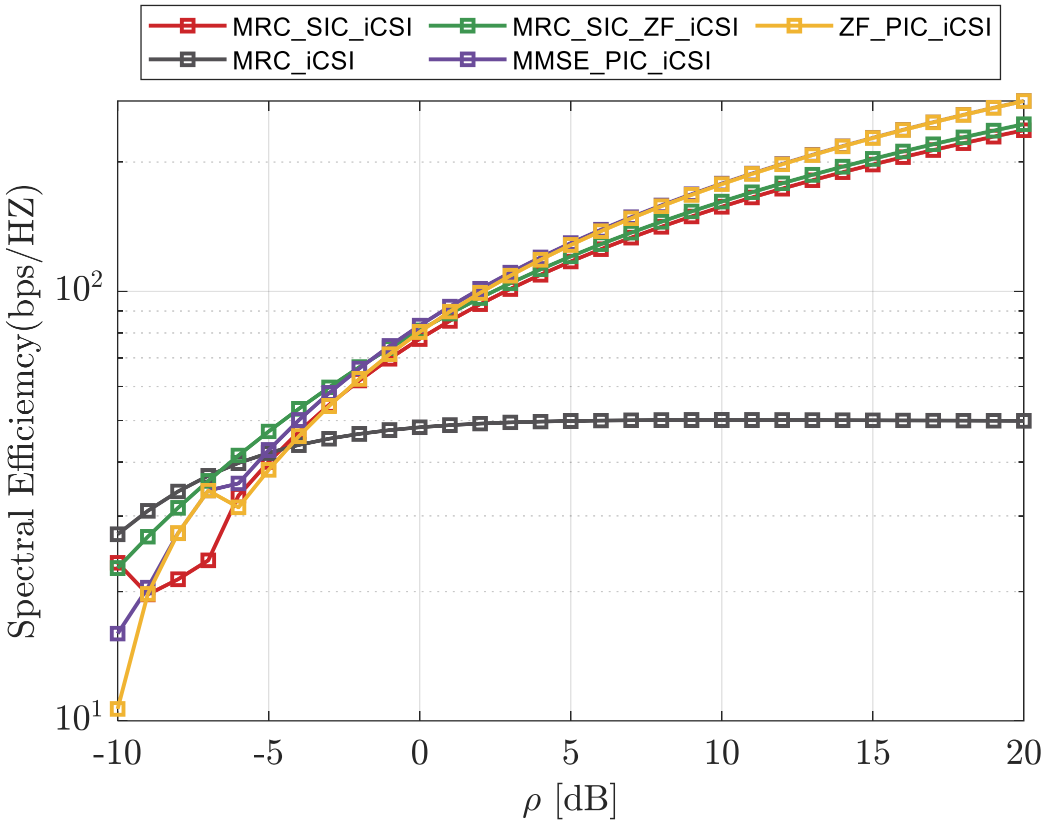

Figure 4.8: Spectral efficiency where K=N=128 imperfect CSI.

4.1.4 The performance of SIC and PIC for the case of K>N

In this scenario, we are assessing the effectiveness of various receivers through the use of SIC and PIC techniques. The results, as depicted in the figure 4.9, indicate that MRC-SIC performs exceptionally well, with lower outage probability values as the SNR increases compared to MRC alone. With both perfect and imperfect CSI, all of the receivers - MRC, MRC-SIC-ZF, MRC-SIC-MMSE, ZF-PIC, and MMSE-PIC - demonstrate comparable performance, except for imperfect CSI of MRC-SIC-ZF, which exhibits lower outage probability than the others.

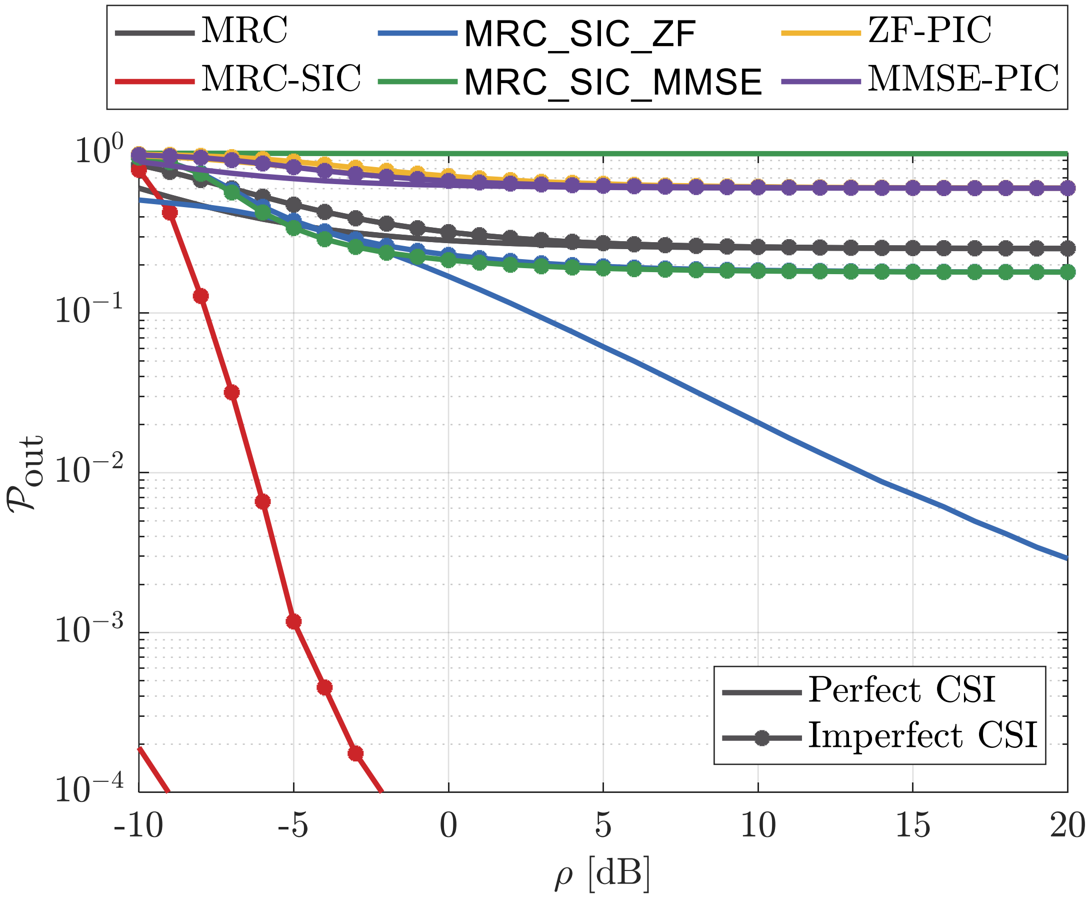

Figure 4. 9: Outage probability versus SNR for N=64, K=128 and r=0.5

The figure 4.10 provides insight into the complexity of each receiver when the number of users exceeds the number of antennas. It shows that MRC and MRC-SIC do not require any matrix inversion, resulting in lower complexity. In contrast, MRC-SIC-MMSE involves only one matrix inversion, while MRC-SIC-ZF, ZF-PIC, and MMSE-PIC require a significantly higher average number of matrix inversions, indicating higher complexity.

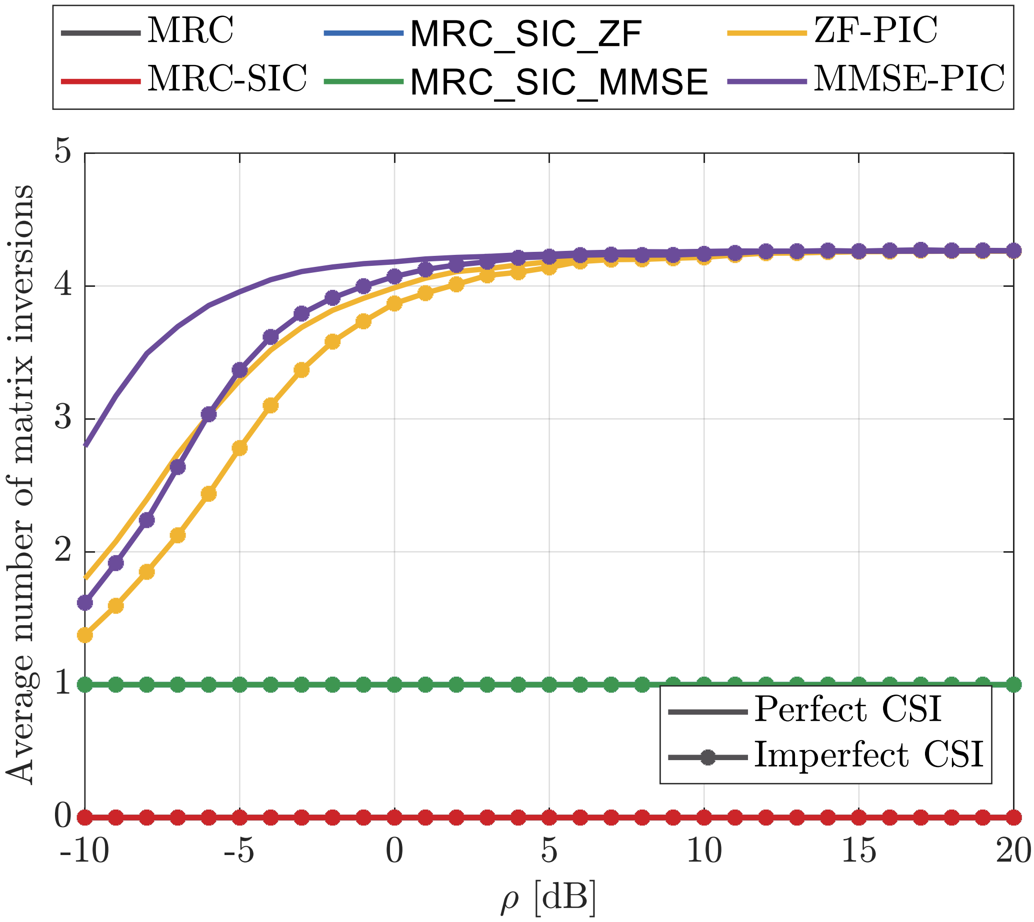

Figure 4. 10: average number of matrix inversion when N=64, K=128 and r=0.5

The figure 4.11 shows the average number of SIC operations for the MRC and MMSE schemes. It should be noted in the figure below the average number of SIC operations for the MRC and MMSE is zero, as no SIC operation is performed. The results indicate that the MRC-SIC scheme exhibits the highest complexity among the receivers considered, as it requires the highest average number of SIC operations. Conversely, the MMSE scheme has the lowest complexity, as the average number of SIC operations performed is zero.

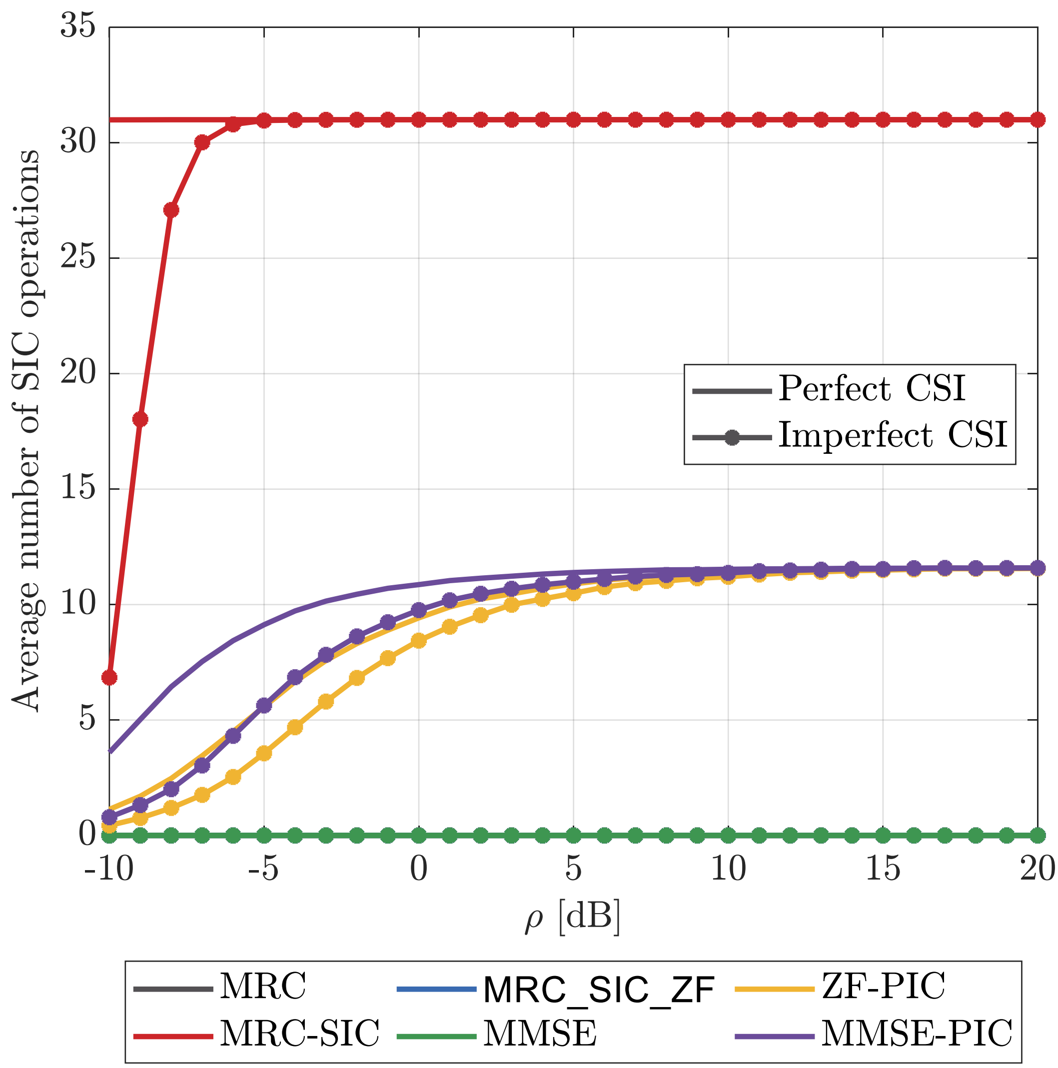

Figure 4. 11:Average number of SIC operation with N=64, K=128 and r=0.5

4.1.5 Spectral efficiency for the condition where K>N,

For perfect CSI, for number of users are greater than number of antenna, MRC_SIC over performs than that of MMSE_PIC. When there are more users than antennas in a MIMO system with perfect CSI, MMSE detector with SIC may not be able to cancel all interference between users due to limited degrees of freedom. However, MRC detector with SIC, which uses signal power to separate users, can effectively cancel interference even with limited degrees of freedom. Therefore, MRC_SIC may outperform MMSE_PIC in such scenarios. MRC_SIC is simpler, while MMSE_PIC is more complex and considers both signal power and interference. When there are more users than antennas, MRC_SIC may be more effective, leading to better performance.

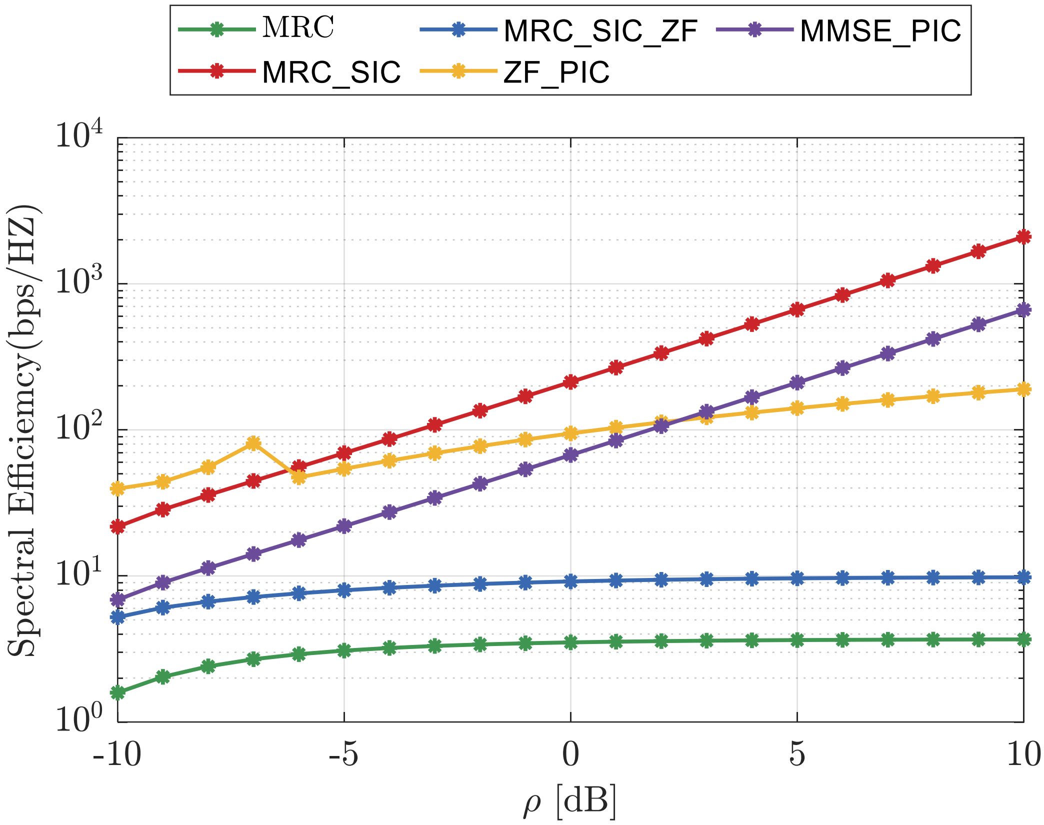

Figure 4. 12:Spectral efficiency where K>N,r=1 in perfect CSI.

In imperfect CSI scenarios, receiver performance in wireless communication systems can vary, especially when SNR is low due to noise and channel estimation errors. MRC alone has low spectral efficiency, whereas MRC_SIC has higher spectral efficiency because it cancels interference. MMSE_PIC and ZF_PIC can also perform poorly at low SNR due to errors in channel estimation. Overall, MRC_SIC has higher spectral efficiency in imperfect CSI scenarios compared to other receivers, but MMSE_PIC, MRC_SIC, and ZF_PIC may be unstable at low SNR.

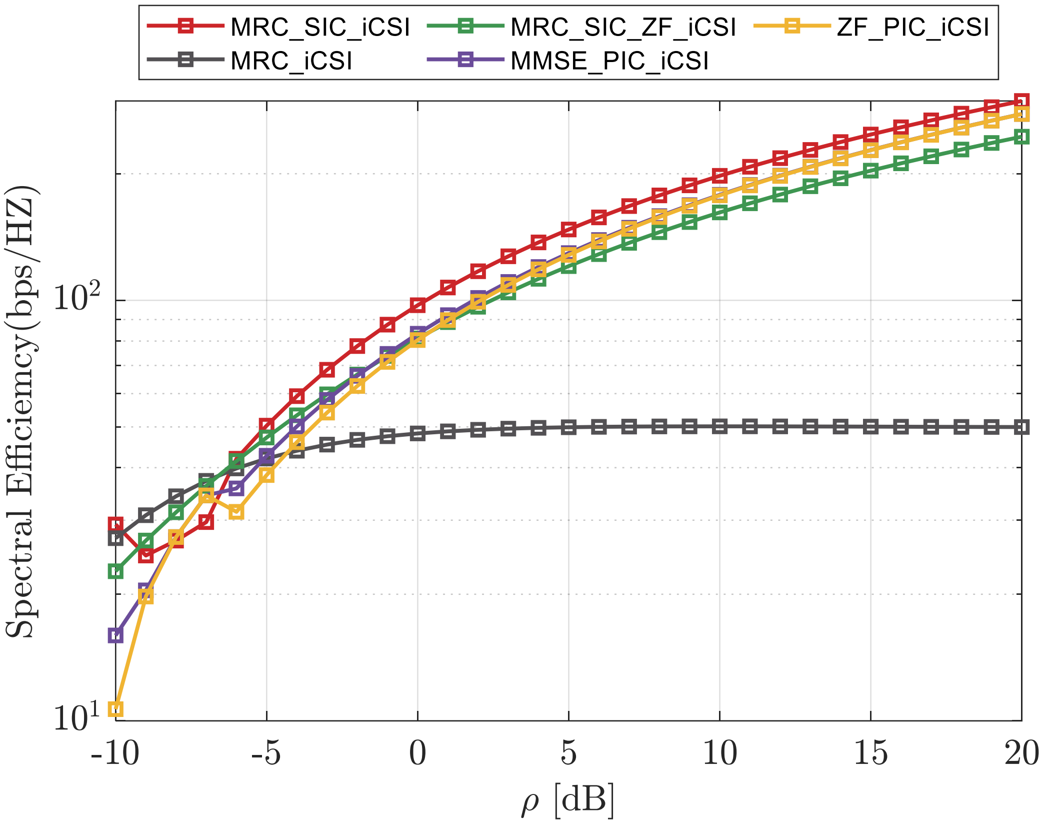

Figure 4. 13:Spectral efficiency where K>N=1 in imperfect CSI.

4.1.6 Performance of SIC and PIC decoding with receivers

In this section, we evaluate the performance of two linear receivers, the zero-forcing (ZF) and minimum mean squared error (MMSE), with two interference cancellation techniques, SIC and PIC. Both the MMSE and ZF receivers require matrix inversion operations during their signal processing.

The evaluation is done by computing the outage probability, which represents the probability of the wireless system failing to transmit data correctly due to noise or interference. The result in figure 4.10 show that the MMSE-SIC and MMSE-PIC receivers have a lower outage probability than the ZF-SIC and ZF-PIC receivers when the channel state information (CSI) is perfect. This suggests that the MMSE receivers are better at mitigating interference and noise than the ZF receivers, particularly in the presence of perfect CSI.

Moreover, the results indicate that the performance of the MMSE-SIC and MMSE-PIC receivers are similar when the system has N=K=64 antennas and devices. However, in the case of the ZF receiver, the ZF-PIC has a lower outage probability than the ZF-SIC. This implies that the PIC technique is more effective than the SIC technique for the ZF receiver, especially when there is noise and interference.

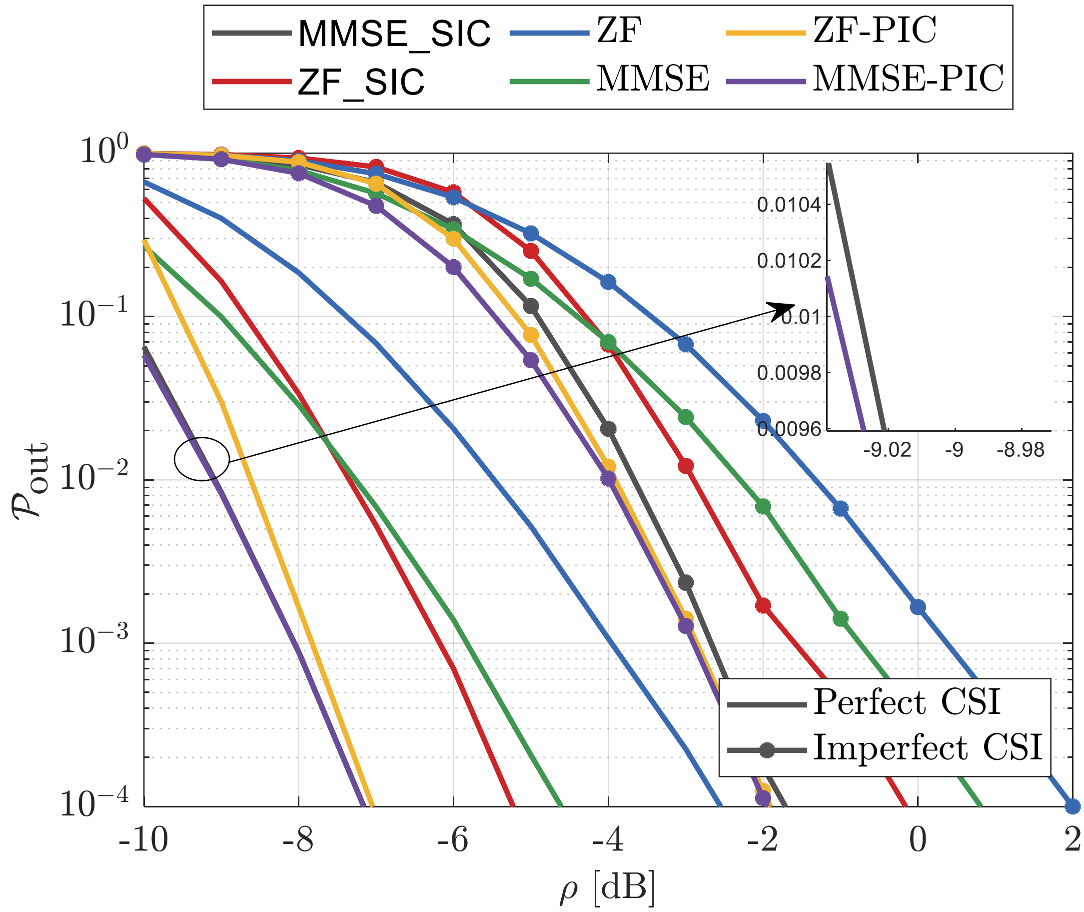

Figure 4. 14: comparison of SIC and PIC performance with ZF and MMSE linear receivers for K=N=64

4.1.7 Performance of the Proposed Method

In Figure 4.15, it has been observed that the minimum mean square error detector with QR decomposition (MMSE_PIC_QR) has a higher spectral efficiency than the standard MMSE_PIC receiver. This can be attributed to the fact that QR decomposition is a more efficient method for solving linear equations compared to the standard method used in MMSE_PIC. QR decomposition reduces the number of calculations required to solve the linear equations, which results in faster and more accurate channel estimation. This improved channel estimation leads to better interference cancellation and higher spectral efficiency for MMSE_PIC_QR compared to MMSE_PIC.

Furthermore, MMSE_PIC_QR is less sensitive to channel variations than MMSE_PIC, which means that it can maintain high spectral efficiency even in scenarios with rapidly changing channels. This makes MMSE_PIC_QR a more robust receiver compared to MMSE_PIC.

It has been observed that ZF_PIC_QR, which uses QR decomposition for channel estimation, has a lower outage probability compared to the standard ZF_PIC receiver. This is because QR decomposition is a more efficient method for solving linear equations, resulting in more accurate channel estimation and better interference cancellation. Additionally, ZF_PIC_QR is less affected by rapidly changing channels, making it a more robust receiver compared to ZF_PIC. Overall, the improved channel estimation provided by QR decomposition leads to better interference cancellation and a lower outage probability for ZF_PIC_QR.

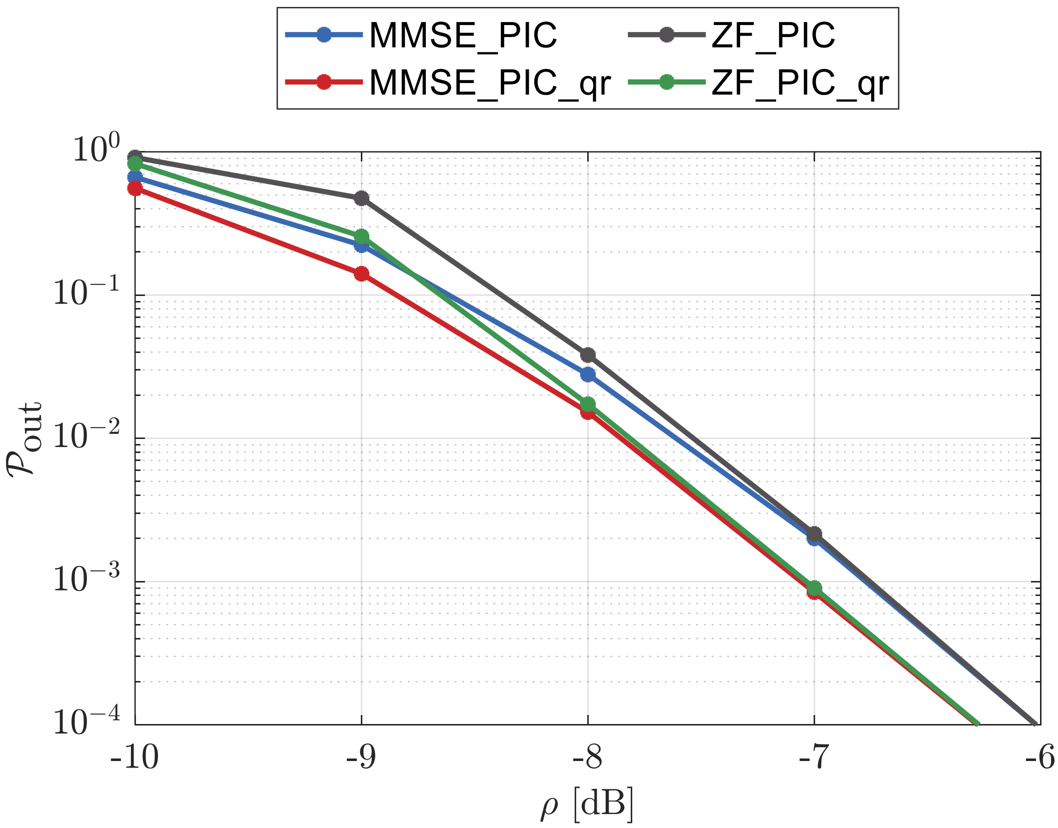

Figure 4. 15 MMSE_PIC_QR

CHAPTER FIVE

5. CONCLUSION AND RECOMMENDATION

5.1 Conclusion

The performance evaluation of different linear and combined receivers in massive MIMO NOMA systems has provided valuable insights into the trade-offs between performance and complexity. The evaluation considered several receivers, including MRC, MRC-SIC, ZF, MMSE, ZF-PIC, and MMSE-PIC, under perfect and imperfect CSI assumptions. The study considers the outage probability, spectral efficiency and computational complexity of the receivers. The results show that the MMSE-PIC receiver is the best performing receiver from existing receivers and it is improved by MMSE_PIC_QR for scenarios where the number of receive antennas is equal to the number of active users (N=K), whereas the MRC-SIC receiver has the best performance when N<K. The evaluation also demonstrates that the perfect CSI receivers outperform the imperfect CSI receivers, and that the average number of matrix inversions. In order to decrease the outage probability of the receivers QR decomposition is also introduced. The results indicate that increasing the number of antennas in massive MIMO systems can decrease the outage probability, indicating better performance, but also increases the computational complexity of the system. However, the complexity of linear receivers can be reduced as the SNR increases. The MMSE receivers, both MMSE-SIC and MMSE-PIC, are better at mitigating interference and noise than the ZF receivers, particularly in the presence of perfect CSI. This is because the MMSE receivers are designed to minimize the mean-squared error between the received signal and the estimated signal, which can effectively mitigate interference and noise.

5.2 Recommendation

The performance of wireless communication systems can be significantly affected by the channel conditions through which the signal travels. Therefore, investigating the performance of massive MIMO NOMA systems under different channel conditions, such as Rician fading or Nakagami-m fading, would provide valuable insights into how these systems perform in different environments. This research could help identify the strengths and limitations of these systems in different scenarios and provide insights into how they perform in practical scenarios. Furthermore, the use of machine learning techniques has shown promise in improving the performance of wireless communication systems. Therefore, exploring the potential of using machine learning techniques to improve the performance of massive MIMO NOMA systems would be a promising area of research. Machine learning techniques could be used to optimize the decoding process in NOMA, improve the accuracy of the channel state information, or enhance the performance of the linear receivers used in these systems. This research could help identify new ways to improve the spectral efficiency of wireless communication systems and pave the way for the development of more advanced communication technologies.

REFERENCE

Al Soufy, K. A. M., Nashwan, F. M. A., Al-Kamali, F. S., & Al-aroomi, S. A. (2023). Performance analysis of linear detection for uplink massive MIMO system based on spectral and energy efficiency with Rayleigh fading channels in 3D plotting pattern. *The Journal of Engineering*, *2023*(4), e12266. https://doi.org/10.1049/tje2.12266

Albdran, S., Alshammari, A., & Matin, M. A. (2017). Spectral and energy efficiency for massive MIMO systems using exponential correlation model. *2017 IEEE 7th Annual Computing and Communication Workshop and Conference (CCWC)*, 1–5. https://doi.org/10.1109/CCWC.2017.7868390

Albreem, M. A., Habbash, A. H. A., Abu-Hudrouss, A. M., & Ikki, S. S. (2021). Overview of Precoding Techniques for Massive MIMO. *IEEE Access*, *9*, 60764–60801. https://doi.org/10.1109/ACCESS.2021.3073325

Al-Hussaibi, W. A., & Ali, F. H. (2019). Performance-Complexity Tradeoffs of MIMO-NOMA Receivers Towards Green Wireless Networks. *2019 IEEE 30th Annual International Symposium on Personal, Indoor and Mobile Radio Communications (PIMRC)*, 1–6. https://doi.org/10.1109/PIMRC.2019.8904383

Beiranvand, J., & Meghdadi, H. (2018). Analytical Performance Evaluation of MRC Receivers in Massive MIMO Systems. *IEEE Access*, *6*, 53226–53234. https://doi.org/10.1109/ACCESS.2018.2866795

Budhiraja, I., Kumar, N., Tyagi, S., Tanwar, S., Han, Z., Piran, Md. J., & Suh, D. Y. (2021). A Systematic Review on NOMA Variants for 5G and Beyond. *IEEE Access*, *9*, 85573–85644. https://doi.org/10.1109/ACCESS.2021.3081601

Chataut, R., & Akl, R. (2020). Massive MIMO Systems for 5G and beyond Networks—Overview, Recent Trends, Challenges, and Future Research Direction. *Sensors*, *20*(10), Article 10. https://doi.org/10.3390/s20102753

Chi, Y., Liu, L., Song, G., Yuen, C., Guan, Y. L., & Li, Y. (2018). Practical MIMO-NOMA: Low Complexity and Capacity-Approaching Solution. *IEEE Transactions on Wireless Communications*, *17*(9), 6251–6264. https://doi.org/10.1109/TWC.2018.2858222

Ding, Z., & Poor, H. V. (2016). Design of Massive-MIMO-NOMA With Limited Feedback. *IEEE Signal Processing Letters*, *23*(5), 629–633. https://doi.org/10.1109/LSP.2016.2543025

Eraslan, E., Daneshrad, B., & Lou, C.-Y. (2013). Performance Indicator for MIMO MMSE Receivers in the Presence of Channel Estimation Error. *IEEE Wireless Communications Letters*, *2*(2), 211–214. https://doi.org/10.1109/WCL.2013.012513.120824

Evolution of Mobile Communication Network: From 1G to 4G - IJMCR. (n.d.). Retrieved May 5, 2023, from http://ijmcr.com/evolution-of-mobile-communication-network-from-1g-to-4g/

Fang, D., Qian, Y., & Hu, R. Q. (2018). Security Requirement and Standards for 4G and 5G Wireless Systems. *GetMobile: Mobile Computing and Communications*, *22*(1), 15–20. https://doi.org/10.1145/3229316.3229322

Ghafoor, U., Ali, M., Khan, H. Z., Siddiqui, A. M., & Naeem, M. (2022). NOMA and future 5G & B5G wireless networks: A paradigm. *Journal of Network and Computer Applications*, *204*, 103413. https://doi.org/10.1016/j.jnca.2022.103413

Ghosh, A., Maeder, A., Baker, M., & Chandramouli, D. (2019). 5G Evolution: A View on 5G Cellular Technology Beyond 3GPP Release 15. *IEEE Access*, *7*, 127639–127651. https://doi.org/10.1109/ACCESS.2019.2939938

Glisic, S., & Makela, J. (2006). Advanced Wireless Networks: 4G Technologies. *2006 IEEE Ninth International Symposium on Spread Spectrum Techniques and Applications*, 442–446. https://doi.org/10.1109/ISSSTA.2006.311811

Goldsmith, A. J., & Varaiya, P. P. (1997). Capacity of fading channels with channel side information. *IEEE Transactions on Information Theory*, *43*(6), 1986–1992. https://doi.org/10.1109/18.641562

Gupta, A., & Jha, R. K. (2015). A Survey of 5G Network: Architecture and Emerging Technologies. *IEEE Access*, *3*, 1206–1232. https://doi.org/10.1109/ACCESS.2015.2461602

Huang, T.-J. (2020). Theoretical Analysis of NOMA Within Massive MIMO Systems. *Wireless Personal Communications*, *112*(2), 777–783. https://doi.org/10.1007/s11277-020-07073-z

Hussain, M., & Rasheed, H. (2020). Nonorthogonal Multiple Access for Next-Generation Mobile Networks: A Technical Aspect for Research Direction. *Wireless Communications and Mobile Computing*, *2020*, 1–17. https://doi.org/10.1155/2020/8845371

Islam, S. M. R., Zeng, M., Dobre, O. A., & Kwak, K.-S. (2018). Resource Allocation for Downlink NOMA Systems: Key Techniques and Open Issues. *IEEE Wireless Communications*, *25*(2), 40–47. https://doi.org/10.1109/MWC.2018.1700099

Iswarya, N., & Jayashree, L. S. (2021). A Survey on Successive Interference Cancellation Schemes in Non-Orthogonal Multiple Access for Future Radio Access. *Wireless*

Personal Communications, *120*(2), 1057–1078. https://doi.org/10.1007/s11277-021-08504-1

Jumaah, A., & Qasim, A. (2022, August 17). *Hybrid Beamforming for Massive MIMO In 5G Wireless Networks*.

Khan, W. U., Li, X., Ihsan, A., Ali, Z., Elhalawany, B. M., & Sidhu, G. A. S. (2021). Energy efficiency maximization for beyond 5G NOMA-enabled heterogeneous networks. *Peer-to-Peer Networking and Applications*, *14*(5), 3250–3264. https://doi.org/10.1007/s12083-021-01176-5

Kim, B., Chung, W., Lim, S., Suh, S., Kwun, J., Choi, S., & Hong, D. (2015). Uplink NOMA with Multi-Antenna. *2015 IEEE 81st Vehicular Technology Conference (VTC Spring)*, 1–5. https://doi.org/10.1109/VTCSpring.2015.7146149

Larsson, E. G., & Van der Perre, L. (2017). *Massive MIMO for 5G*.

Le, M. T. P., Sanguinetti, L., Bjornson, E., & Benedetto, M.-G. D. (2019). What is the Benefit of Code-domain NOMA in Massive MIMO? *2019 IEEE 30th Annual International Symposium on Personal, Indoor and Mobile Radio Communications (PIMRC)*, 1–5. https://doi.org/10.1109/PIMRC.2019.8904268

Li, X., Gani, A., Salleh, R., & Zakaria, O. (2009). *The Future of Mobile Wireless Communication Networks* (p. 557). https://doi.org/10.1109/ICCSN.2009.105

Liu, M., Zhang, J., Xu, C., Ding, Z., & Wu, Y. (2016, September 18). *Non-asymptotic Outage Probability of Large-scale MU-MIMO Systems with Linear Receivers*. https://doi.org/10.1109/VTCFall.2016.7881109

Liu, Y., Qin, Z., Elkashlan, M., Nallanathan, A., & McCann, J. A. (n.d.). *Non-orthogonal Multiple Access in Hybrid Heterogeneous Networks*.

Ma, J., Liang, C., Xu, C., & Ping, L. (2017). On Orthogonal and Superimposed Pilot Schemes in Massive MIMO NOMA Systems. *IEEE Journal on Selected Areas in Communications*, *35*(12), 2696–2707. https://doi.org/10.1109/JSAC.2017.2726019

Ruzomberka, E., Love, D. J., Brinton, C. G., Gupta, A., Wang, C.-C., & Poor, H. V. (2023). *Challenges and Opportunities for Beyond-5G Wireless Security* (arXiv:2303.00727). arXiv. http://arxiv.org/abs/2303.00727

Senel, K., Cheng, H. V., Björnson, E., & Larsson, E. G. (2019). What Role can NOMA Play in Massive MIMO? *IEEE Journal of Selected Topics in Signal Processing*, *13*(3), 597–611. https://doi.org/10.1109/JSTSP.2019.2899252

Shaikh, A., & Kaur, M. J. (2019). Comprehensive Survey of Massive MIMO for 5G Communications. *2019 Advances in Science and Engineering Technology International Conferences (ASET)*, 1–5. https://doi.org/10.1109/ICASET.2019.8714426

Shi, Z., Yang, G., Fu, Y., Wang, H., & Ma, S. (2022). *Performance Analysis of MIMO-NOMA Systems with Randomly Deployed Users*.

Shlezinger, N., Alexandropoulos, G. C., Imani, M. F., Eldar, Y. C., & Smith, D. R. (2021). Dynamic Metasurface Antennas for 6G Extreme Massive MIMO Communications. *IEEE Wireless Communications*, *28*(2), 106–113. https://doi.org/10.1109/MWC.001.2000267

Tabassum, H., Ali, Md. S., Hossain, E., Hossain, Md. J., & Kim, D. I. (2017). Uplink Vs. Downlink NOMA in Cellular Networks: Challenges and Research Directions. *2017 IEEE 85th Vehicular Technology Conference (VTC Spring)*, 1–7. https://doi.org/10.1109/VTCSpring.2017.8108691

Tominaga, E. N., López, O. L. A., Alves, H., Souza, R. D., & Rebelatto, J. L. (2022). Performance Analysis of MIMO-NOMA Iterative Receivers for Massive

Connectivity. *IEEE Access*, *10*, 46808–46822. https://doi.org/10.1109/ACCESS.2022.3170715

Toward Massive Machine Type Cellular Communications | IEEE Journals & Magazine | IEEE Xplore. (n.d.). Retrieved May 5, 2023, from https://ieeexplore.ieee.org/document/7736615

Tullberg, H., Popovski, P., Li, Z., Uusitalo, M. A., Hoglund, A., Bulakci, O., Fallgren, M., & Monserrat, J. F. (2016). The METIS 5G System Concept: Meeting the 5G Requirements. *IEEE Communications Magazine*, *54*(12), 132–139. https://doi.org/10.1109/MCOM.2016.1500799CM

Uddin, M. B., Sarkar, M., Faisal, K. N., & Ali, M. M. (2014). *Performance analysis of Nakagami-m fading massive MIMO channels with linear receivers*. https://doi.org/10.1109/ICCITechn.2014.7073089

Wang, H., Dong, J., Tang, K., & Shi, H. (2021). Outage Performance Analysis of NOMA in Wireless Powered Cognitive Radio Networks with AF and DF Relaying Techniques. *Entropy*, *23*(11), Article 11. https://doi.org/10.3390/e23111463

Wang, S., Chen, L., Chen, X., & Wei, G. (2017). Performance analysis of ultra-dense networks with MRC reception and successive interference cancellation under rate-limited backhaul. *International Journal of Communication Systems*, *30*(6), e3116. https://doi.org/10.1002/dac.3116

Wei, X., Xiang, L., Cottatellucci, L., Jiang, T., & Schober, R. (2019). Cache-Aided Massive MIMO: Linear Precoding Design and Performance Analysis. *ICC 2019 - 2019 IEEE International Conference on Communications (ICC)*, 1–7. https://doi.org/10.1109/ICC.2019.8761126

Wu, J. (2018). Research on Massive MIMO Key Technology in 5G. *IOP Conference Series: Materials Science and Engineering*, *466*(1), 012083. https://doi.org/10.1088/1757-899X/466/1/012083

Yiping, C., & Yuhang, Y. (2007). A new 4G architecture providing multimode terminals always best connected services. *IEEE Wireless Communications*, *14*(2), 36–41. https://doi.org/10.1109/MWC.2007.358962

Zhang, D., Liu, Y., Ding, Z., Zhou, Z., Nallanathan, A., & Sato, T. (2017). Performance Analysis of Non-Regenerative Massive-MIMO-NOMA Relay Systems for 5G. *IEEE Transactions on Communications*, *65*(11), 4777–4790. https://doi.org/10.1109/TCOMM.2017.2739728

Zhu, X., Meng, Z., Xie, J., Tu, X., & Zeng, W. (2019). Performance Analysis of Linear Precoding in Massive MIMO Systems With Finite-Alphabet Inputs. *IEEE Access*, *7*, 85696–85704. https://doi.org/10.1109/ACCESS.2019.2925939